Quantitative mapping of mRNA 3' ends in *Pseudomonas aeruginosa* reveals a pervasive role for premature 3' end formation in response to azithromycin

Salini Konikkat[1], Michelle R. Scribner[2], Rory Eutsey[1], N. Luisa Hiller[1], Vaughn S. Cooper[2], C. Joel McManus[1]
[1] Department of Biological Sciences, Carnegie Mellon University, Pittsburgh, USA;
[2]Department of Microbiology and Molecular Genetics, University of Pittsburgh, Pittsburgh, USA

ABSTRACT

Pseudomonas aeruginosa produces serious chronic infections in hospitalized patients and immunocompromised individuals, including patients with cystic fibrosis. The molecular mechanisms by which *P. aeruginosa* responds to antibiotics and other stresses to promote persistent infections may provide new avenues for therapeutic intervention. Azithromycin (AZM), an antibiotic frequently used in cystic fibrosis treatment, is thought to improve clinical outcomes through a number of mechanisms including impaired biofilm growth and quorum sensing (QS). The mechanisms underlying the transcriptional response to AZM remain unclear. Here, we interrogated the *P. aeruginosa* transcriptional response to AZM using a fast, cost-effective genome-wide approach to quantitate RNA 3' ends (3pMap). We also identified hundreds of *P. aeruginosa* genes with high incidence of premature 3' end formation indicative of riboregulation in their transcript leaders using 3pMap. AZM treatment of planktonic and biofilm cultures alters the expression of hundreds of genes, including those involved in QS, biofilm formation, and virulence. Strikingly, most genes downregulated by AZM in biofilms had increased levels of intragenic 3' ends indicating premature transcription termination, transcriptional pausing, or accumulation of stable intermediates resulting from the action of nucleases. Reciprocally, AZM reduced premature intragenic 3' end termini in many upregulated genes. Most notably, reduced termination accompanied robust induction of *obgE*, a GTPase involved in persister formation in *P. aeruginosa*. Our results support a model in which AZM-induced changes in 3' end formation alter the expression of central regulators which in turn impairs the expression of QS, biofilm formation and stress response genes, while upregulating genes associated with persistence.

INTRODUCTION

The Gram-negative bacterium *Pseudomonas aeruginosa* (*P. aeruginosa*) is an important opportunistic pathogen in humans. It is a leading cause of hospital-associated pneumonia [1-6]. *P. aeruginosa* infections are associated with increased morbidity and risk of death in patients with pulmonary disorders such as cystic fibrosis (CF), chronic obstructive pulmonary disease (COPD), and diffuse parabronchiolitis (DPB). *P. aeruginosa* readily forms aggregates or biofilms that are thought to exacerbate disease progression, and contribute to antibiotic resistance and the persistent nature of *P. aeruginosa* infections [7-11]. For example, in the lungs of patients with cystic fibrosis, *P. aeruginosa* biofilms cause continual damage to the airways by recurrent infection, inflammation, and airway obstruction [12]. Due to their clinical importance, understanding the regulation of biofilms has become a major focus of *P. aeruginosa* research.

Sub-inhibitory concentrations of the macrolide antibiotic azithromycin (AZM) improves clinical outcomes in patients with cystic fibrosis, diffuse panbronchiolitis (DPB) and chronic obstructive pulmonary disease (COPD) [13-17]. In mouse models of *P. aeruginosa* infection, including a CF model, AZM reduced bacterial load and improved lung pathology [18,19]. These effects were attributed to the interference with quorum sensing (QS), suppression of virulence factors, and attenuation of host inflammatory responses. Previous studies demonstrated that AZM targets QS by an uncertain mechanism, which in turn is proposed to control biofilm formation and virulence factor production [20-29]**.** Consistent with these biological effects, AZM treatment changes the transcript levels of genes involved in QS, virulence factor production, and oxidative stress [2,20-29]**.** For example, AZM downregulates the expression of components of the *lasI/lasR* and *rhlI/rhlR* QS systems as well as QS-controlled genes coding for virulence factors such as elastase, flagellar motility factors, and rhamnolipid synthesis [2,20-22,25,27-29]**.** AZM also downregulates QS-regulated oxidative stress response genes including catalase *katA* and superoxide dismutase *sodB* [25,30]**.** While these pathways clearly respond to AZM, the underlying mechanisms remain unclear, particularly in biofilms.

AZM binds near the peptidyl transferase center on the large subunit of bacterial ribosomes and disrupts translation elongation by hindering the passage of newly synthesized polypeptides through the polypeptide exit tunnel [31-35]**.** Translation inhibition is hence thought to account for QS inhibition, which in turn inhibits biofilm formation and virulence

gene expression by AZM in *P. aeruginosa*. Because transcription elongation and mRNA translation are spatio-temporally coupled in bacteria [36-39], the translation stalling caused by AZM could directly alter the production of full-length transcripts from QS genes and transcriptional regulators of the stress response. The extent of reduced transcriptional processivity due to AZM treatment remains an important unresolved question because methods used in previous studies lacked the resolution to differentiate between premature and full-length mRNA transcripts.

RNA 3' end mapping allows genome-wide identification of RNA 3'-OH ends [40] and quantitation of differential gene expression [41,42]. RNA molecules with free 3'-OH ends include both full length or premature transcripts resulting from intrinsic or factor-dependent transcription termination, transcriptional pauses and stable intermediates resulting from ribonucleases [40,43-45]. Bacteria often employ conditional transcription termination in their transcript leaders to regulate expression in response to drugs, metabolites, and stresses [46-51]. *Cis*-regulatory elements that use premature transcription termination include transcription attenuators and riboswitches, often collectively referred to as riboregulators. Their mechanisms of action involve formation of alternate RNA structures that promote full length transcript synthesis (anti-terminator) or effect premature transcription termination (terminator). The activities of riboregulators are often mediated by interaction of the nascent transcript with small molecules, ribosomes, tRNAs, or regulatory proteins. As such, riboregulators are potential therapeutic targets, and may provide synthetic biology applications [52-55]. Since conditional premature transcription termination regulates biofilm formation, virulence, and expression of antibiotic resistance genes in other bacteria [40,51,56,57], efforts to identify and characterize genes likely to be controlled by riboregulators in *P. aeruginosa* would be beneficial.

In this study, we employed a modification of genome-wide 3' end mapping approach Term-Seq [40], which we call 3pMap (Figure 1), to characterize the transcriptional landscape of *P. aeruginosa* and the acute effects of clinically relevant sub-inhibitory concentrations of AZM on gene expression. We examined differential gene expression in planktonic and biofilm cultures of *P. aeruginosa* in response to AZM. AZM altered the expression of over two hundred genes in each condition, including key factors involved in QS, biofilm formation, virulence factor production, and stress responses. Notably, most genes downregulated in response to AZM in biofilms showed increased intragenic 3' end formation, indicating a role for the antibiotic in regulating transcription. Furthermore, AZM treatment strongly induced the

94 peristence gene *obgE* [61], accompanied by a corresponding decrease in premature 3' end
95 formation in its transcript leader. Together, our results provide novel insights into
96 transcriptional regulation in *P. aeruginosa*, and support a model in which AZM-induced
97 changes in premature 3' end formation alter the expression of key transcriptional modulators
98 and structural genes involved in QS, virulence, stress response, and persistence.

99 METHODS

100 Strains and culture conditions

101 The effects of AZM on both planktonic cells and biofilms of a UCBPP-PA14 strain isolate
102 (genome at NCBI GEO under accession GSE173073) were investigated. Populations from
103 freezer stock were revived by culturing overnight in LB broth at 37ºC with shaking at 300
104 RPM to an optical density (OD_{600}) of 1.0. For planktonic cells, this culture was diluted to OD_{600}
105 0.1 in 5 mL LB broth and grown to a final OD_{600} of 0.47 (~3 hours shaking at 37ºC). A
106 subinhibitory concentration of AZM (0.5 µg/ml final concentration) was added to three
107 cultures (Supplementary Figure S1). Three cultures without AZM were used as negative
108 controls. The cultures were incubated for an additional 20 minutes at 37ºC. One volume of
109 RNA stabilization solution (5.3M ammonium sulfate, 20 mM EDTA, 25 mM sodium citrate, pH
110 5.2) was added and the cells were pelleted by centrifugation at 2,500xg for 10 minutes. The
111 supernatants were discarded and the pellets were frozen at -20ºC for RNA extraction. For
112 biofilms, a mid-log phase PA14 culture was diluted to an optical density of 0.05 into six-well
113 plates (one plate per culture) incubated at 37ºC for 24 hours. The media was removed and
114 replaced with or without AZM (0.5 µg/ml) and incubated at 37ºC for 3 hours. The media was
115 removed and 750 µl RNA stabilization solution was added to each well. The biofilms were
116 scraped from the wells and the cells were pelleted by centrifugation at 2500xg for 10 minutes.
117 The supernatants were discarded and samples were saved at -20ºC until RNA extraction.

118 RNA extraction and DNase treatment

119 Total RNA was extracted using the Quick-RNA™Fungal/Bacterial Miniprep kit (Zymo
120 Research R2010) according to the manufacturer's instructions. To remove any contaminating
121 genomic DNA, 20-40 mg of total RNA was incubated with 6 units of TURBO™-DNase
122 (Thermo Fisher Scientific AM2238), 1X TURBO™DNase buffer, and 20 units of SUPERase-
123 In™RNase inhibitor in a 1 ml reaction for 1 hour at 37ºC. The RNA was re-isolated using
124 acid-phenol, ethanol precipitated, and resuspended in nuclease-free water. The absence of

contaminating DNA was confirmed by the absence of a GAPDH PCR product, using genomic DNA as a positive control for the PCR.

HIGH-THROUGHPUT SEQUENCING LIBRARY PREPARATION USING 3pMAP

3'-linker addition and rRNA depletion

To reduce secondary structure, a 5 µl reaction containing 2 µg of RNA and 375 ng of universal miRNA 3'-cloning linker (New England Biolabs S1315S) was heated at 80°C for 2 minutes and placed on ice. The RNA was ligated to the 3'-linker by incubating the mix overnight at 16°C in a 20 µl reaction containing 12.5 % PEG800, 10% DMSO, 1X T4 RNA Ligase buffer, 20 units SUPERase-In™ RNase inhibitor, and 200 units of T4 RNA Ligase 2, truncated K227Q (New England Biolabs M0351S). The RNA was precipitated with 3 volumes of ethanol, 1/10thvolume of 3M sodium acetate (pH 5.2) and 20 µg of glycogen at -80°C for 1 hour. Ribosomal RNA (rRNA) depletion was performed using the Ribo-Zero rRNA removal kit for bacteria (Illumina MRZMB126) as per the manufacturer's instructions, and ethanol precipitated as discussed above.

High-throughput sequencing library synthesis and sequencing

Strand-specific 3pMap libraries were prepared using the QuantSeq Flex Targeted RNA-seq kit (Lexogen SKU:035.24) with the following modifications. Oligonucleotides used for library synthesis are listed below. First strand cDNA synthesis was performed as per the manufacturer's instruction using 5 µl of 2.5 µM custom first strand synthesis primer mix containing partial Illumina Read 1 adapter (below). Following the first strand synthesis, RNA was removed, and the second strand of cDNA was synthesized using SS1X mix and custom second strand synthesis primer with Illumina Read 2 sequence. Half the purified cDNA was used as a template for PCR amplification using barcoded primers provided with the kit. The library concentrations were quantified using a Qubit dsDNA high sensitivity assay (ThermoFisher Scientific Q32854) and sizes were estimated on a Tapestation high sensitivity DNA ScreenTape (Aglient). The libraries were sequenced on an Illumina NextSeq 500 platform in a single-read, 75-nucleotide run as per the manufacturer's instructions.

Oligonucleotides for library preparation

First Strand Synthesis Mix (equimolar mix of three primers used for first strand synthesis):

3PUTR-FS-N-Read1 5'-CACGACGCTCTTCCGATCTNATTGATGGTGCCTACAG-3'

3PUTR-FS-NN-Read1 5'-CACGACGCTCTTCCGATCTNNATTGATGGTGCCTACAG-3'

3PUTR-FS-NNN-Read1 5'-CACGACGCTCTTCCGATCTNNNATTGATGGTGCCTACAG-3'

Random Second Strand Synthesis (SS) Primer

RandomSS-Read2 5'-GTTCAGACGTGTGCTCTTCCGATCTNNNNNNNNNNNN-3'

DATA PROCESSING

Aligning reads to the genome and identifying significant peaks

Reads were first trimmed to remove adapter sequences. 5' ends were trimmed with a custom Perl script (5p-trimmer.pl), which removed 15-17 nucleotides preceding "CAG", then 3' ends were trimmed using Cutadapt (v. 1.9.1; parameters -a AGATCGGAAGAGC -m 25) and aligned to our UCBPP-PA14 genome sequence (NCBI GEO, see above) using Bowtie2 (v 2.1.0, default parameters) to obtain the genomic coordinates for the 3'-ends of reads [58,59]. 3pMap is strand specific, such that reads map to the strand from which they were transcribed. We used a custom Perl script, Map3p-seq-peaks.pl, to compare aligned 3' end locations to an expected Poisson distribution of random 3' ends in 50 nucleotide windows. Candidate peaks required a raw p-value < 5 x 10^-5, > 5-fold more reads than the average within the window, and a minimum of 5 total reads per peak. Strand specific peak files for each replicate were combined and RNA 3' peaks that are present in at least two of three sample replicates were identified using a combination of bedtools functions [60] (MakeSignificantPeaksFile.sh). These peaks are referred to as significant peaks in further analyses.

Bioinformatic prediction of Rho-independent terminators in *P.* aeruginosa

Rho-independent terminators in the *P. aeruginosa* genome were predicted using ARNold, a web-tool that combines two prediction algorithms Erpin and RNAmotif [61]. Due to limitations on the input file size, *P. aeruginosa* genome was split into two halves. The genomic coordinates for predicted Rho-independent terminators in the second output file were compiled using a Python script and a mergebed bedtools operation was performed in a strand-specific manner to obtain a 6-column file with coordinates for Rho-independent terminators (Supplementary Table S1).

Genome-browser images

Integrated Genome Viewer [62] (IGV) images were exported as Scaled Vector Graphics (.svg) images and edited on Adobe Illustrator or Affinity Designer to obtain simplified views.

Views for negative strand genes were inverted using mirror display option for the ease of visualization. IGV tracks show the reads present in the same strand as the gene of interest, using autoscale. The genomic coordinates for the IGV snapshots are included in the images. 3' end read counts for samples are indicated above the tracks corresponding to the sample.

Associating 3' end reads with *P. aeruginosa* genes

For analysing the ability of 3pMap to accurately detect RNA 3' ends, 3' end reads within 400 nucleotides of genes were associated with the coordinates in .gff file using the bedtools windowbed function. The 3' end significant peaks were associated with tRNAs and mRNAs if they were (a) intragenic - located within the gene boundaries or (b) intergenic – n nucleotides downstream of the annotated 3' end and does not overlap into the next gene on the same strand (n=400 for mRNAs, n=100 for tRNAs and mRNAs as the intergenic spaces between these genes and their downstream genes were shorter). For remaining steps in the analysis, genomic coordinates of *P.aeruginosa* transcript leaders (5'-UTRs) and transcriptional unit boundaries were obtained using LiftOver (UCSC genome browser) from a previous study on a nearly identical strain [63,64] (Supplementary Table S2). If the lifted-over transcript leaders encroached the CDS of an upstream PA14 gene, gene boundaries in the PA14 genome annotation were retained. 3' end reads within 400 nucleotides of genes were identified using the bedtools windowbed function (createFilesToAssociateWithGenes.sh). The 3' end reads and peaks were assigned to gene transcriptional units if they satisfied either of the following conditions: a) the read is within defined operon boundaries, b) the read is downstream of the annotated 3' end of a gene and does not overlap more than 10 nucleotides into the next transcriptional unit on the same strand (Gen. The significant peaks associated with transcriptional units are identified in Supplementary Table S3 (SignificantPeaksPerGeneFinder.py).

Quantifying the effects of AZM on gene expression in *P. aeruginosa*

For differential expression, we used total read counts in the 3'-UTR regions of transcriptional units (all 3' reads) other than rRNAs as discussed above. The total number of reads in the 3' UTRs was compiled using a Python script that sums up the counts for reads associated with 3'UTRs of transcriptional units (DEseqFileCreateAndRunInstruction.py), and pairwise differential expression analysis of planktonic and biofilm cultures +/- AZM were performed using DEseq2 [65] (Supplementary Table S5 and S6). Genes with an adjusted P value (pAdj) < 0.1 were considered to have significant expression differences.

Detecting relative changes in premature 3' end formation in the presence of AZM

Since transcription pausing or termination would result in reproducible peaks, we used reads corresponding to significant peaks of transcript ends in the intragenic (I) and 3'UTR regions (FL) of transcription units for protein coding genes for this analysis (IFLratioFileCreator_Step1.py). To avoid false-positives due to low read counts, genes were only analyzed if the majority of the replicates have both I and FL read counts (no more than one zero value for I and / or FL per sample and treatment. Pseudocounts of 1 were used for all remaining zero values from I or FL peaks. Cochran-Mantel-Haenszel tests were used to identify genes with significant differences between the expected and observed read frequencies in triplicate samples of untreated and treated cultures (RcodeCMHIFL.R). The Benjamini-Hochberg procedure was used to control false discovery, with FDR < 0.1. Relative changes in levels of premature transcripts within the coding sequences of genes in response to AZM were estimated as the odds-ratio of intragenic (I) / full length (FL) 3' end peak read counts in AZM treated vs. untreated samples. Tests were performed in R (version 3.6.1) using default parameters in 2 x 2 x 3 matrices.

Predicting RNA regulatory elements that in P*. aeruginosa* transcript leaders

We categorized reads present in the transcript leaders or 0-40 nucleotides into the ORF as early transcript termini reads. Percentage early termini reads (%ET) was calculated as follows:

$$\% \text{ ET} = (\text{Early termini reads} / \text{Total 3' end reads in the gene}) * 100$$

Highest % ET that detected most predicted/known riboswitches (Supplementary Table S11) in *P. aeruginosa* was employed as cut-off (Supplementary Figure S11A) [66-68]. Genes with % ET above the cut-off in at least two replicates were considered for the next step. Since significant peaks denote 3'-ends that are reproducibly present above background noise in at least two replicates, only genes with significant peaks in their early termination zone were considered as outlier candidates. The ability of the RNA sequences upstream of significant peaks to form alternate RNA structures capable of causing Rho-independent termination were analyzed using the PASIFIC (Prediction of Alternative Structures for Identification of *cis*-regulation) web-based application [69]. Sequences were analyzed for the ability to form Rho-independent (intrinsic) terminators using ARNold [61].

247 **RESULTS**

248 **3pMap accurately identifies RNA 3'-OH ends**

249 To investigate transcription-mediated regulatory mechanisms and the acute effects of AZM
250 on the transcriptional landscape of *Pseudomonas aeruginosa,* we developed 3pMap. 3pMap
251 adapts a commercially available RNA-seq kit to map mRNA 3' ends, by ligating a custom 3'
252 end oligonucleotide adapter to total cellular RNA and directing library preparation to the
253 adapter sequence (Figure 1A). Sequencing library synthesis using 3pMap has fewer steps
254 compared to the Term-Seq approach [40] and requires minimal RNA input (2 μg) per sample.

255 We first applied 3pMap to *P. aeruginosa* PA14 grown under planktonic conditions in rich
256 media in triplicate to evaluate its accuracy. We aligned the reads to the genome and identified
257 3' end peaks that are present in at least two replicates of a sample (significant peaks, see
258 Methods). We assessed the distribution of 3' significant peaks in intragenic vs. intergenic
259 regions of three classes of genes – tRNAs and protein coding sequences (Supplementary
260 Figure S2). Greater than 98% of significant peaks associated with tRNA genes were located
261 within 3 nucleotides of the corresponding annotated 3' ends (Supplementary Figure S2A-
262 S2B). Similarly, 88.4% of significant peaks associated with mRNAs were located in intergenic
263 regions, with <12% located within coding sequences ((Supplementary Figure S2C). These
264 results show that 3pMap accurately detects known RNA 3' ends. We detected a small amount
265 of ribosomal rRNAs retained in the samples after rRNA depletion. Alignment of significant
266 peaks assigned to rRNAs confirmed the ability of 3pMap to detect RNA 3' ends accurately,
267 and suggest alternative rRNA 3' ends that may be used in precursor or mature rRNA
268 (Supplementary Figure S2D-S2H). Together, these results illustrate that 3pMap identifies
269 both known and novel RNA 3' ends.

270 Finally, we investigated the relative frequency of 3' ends in Rho-independent terminators. We
271 used ARNOLD to predict Rho-interminators in the *P. aeruginosa* genome (Supplementary
272 Table S1) [61]. ARNOLD predicts Rho-independent terminators bioinformatically using
273 examples from *E. coli* and *B. subtilis*. On average, 18.4% of 3' end reads in significant peaks
274 assigned to protein-coding genes overlapped predicted Rho-independent terminators
275 (Supplementary Table S4). Since RNA 3' ends can be trimmed by nucleases [43], this
276 represents a lower limit of the amount of 3' ends caused by Rho-independent termination.
277 Thus, we estimate that roughly one fifth of 3' ends are generated by Rho-independent
278 termination in *P. aeruginosa*, suggesting a substantial role for Rho-dependent termination.

The effects of AZM on *P. aeruginosa* gene expression

We next investigated how AZM alters gene expression in *P. aeruginosa*, since bacterial transcription and translation are coupled [36-39]. To understand the acute response of *P. aeruginosa* to AZM, planktonic and biofilm cultures were treated with the antibiotic for 20 minutes and 3 hours, respectively. We utilized the published transcript start sites from a nearly identical strain to define transcript leaders in the strain used in this study by converting genome coordinates with liftOver (Supplementary Table S2) [63].To assess gene expression changes in response to AZM, we performed differential expression analysis (DEseq2) using all reads from 3' UTR regions of transcriptional units (Methods; Figure 1C, Figure 2A and Figure 2B, and Supplementary Table S5-S6) with an FDR of 10% (Supplementary Table S7). In AZM-treated planktonic cultures, 209 and 68 genes showed more than two-fold up- or down-regulation, respectively (Figure 3C). In biofilm cultures, 168 genes were downregulated and 112 genes were upregulated more than two-fold (Supplementary Table S7, Figure 2C). We observe little overlap between expression changes in planktonic and biofilm cultures, potentially due to a combination of differences in the duration of AZM treatment and lifestyle-specific gene expression patterns.

In AZM treated biofilms (Figure 2D), we observed reduced transcript levels of several global gene expression modulators associated with stress responses (*rpoS* [70,71], *rpoH* [72], and *relA* [73]), anaerobic metabolism (*anr* [74,75]), virulence and biofilm formation (*rsmY* [76]), amino acid and nitrogen metabolism (*argR* [77]), *ntrBC* and *gdhB* [78]), QS (*vqsR* [79]), and antibiotic resistance (*amgR* [80]) (Figure 3D). The expression of stress, virulence, biofilm, motility, and metabolism-related genes, many of which are controlled by these regulators, were also downregulated. In contrast, AZM treatment in biofilms upregulated expression of the *obgE* GTPase (also known as CgtA) more than 20-fold. Previous work suggests that ObgE is a key player in the stringent response and promotes bacterial persistence [81,82]. Overall, the functional categories in which multiple genes were differentially expressed here - inhibition of biofilm formation, AHL quorum sensing regulons, virulence, and stress responses - are broadly consistent with previously reported effects of AZM on *P. aeruginosa* [18,24,25,28]. However, our results better define several genetic pathways that may underlie these changes, including those producing the stringent response (Figure 2D).

In planktonic cells, AZM also downregulated the expression of global gene expression modulators *rpoS* [70,71], *vqsR* [79], and *algR* [83], and promoted early transcription

311 termination (Supplementary Table S7), but not significant downregulation, of *lasI*. As in
312 biofilms, virulence factor genes were downregulated, though different genes were impacted
313 (Figure 3E). These include phenazine biosynthesis genes *phzB2-G2* and *phzM* [84], *aprA*
314 [85]*, and rahU* [86]. Pilus genes *fimU* and *pilWXY1* were also downregulated, as were several
315 heat shock proteins (*groEL, groES,* and *ibpA*, and *dnaK* [87-90]). *mvfR (pqsR)*, a regulator of
316 PQS quorum sensing [91], was upregulated, as was *obgE* though to a lesser extent than in
317 biofilms (1.96-fold). In contrast to the biofilm samples, many genes associated with biofilm
318 formation including *pelABCDEFG, gacA,* and the Wsp pathway were found to be upregulated
319 upon AZM treatment, as well as haem biosynthesis proteins *hemL* and *hemE* [92-95]. The
320 upregulation of biofilm genes is in contrast to previous studies and potentially reflects the
321 relatively shorter duration of AZM treatment we employed or other differences in growth
322 conditions.
323 We leveraged 3pMap data to evaluate differential changes in the levels of 3' OH ends
324 associated with tRNAs in response to AZM. Charged tRNA carry cognate amino acids at their
325 3' ends, while uncharged tRNA have free 3' OH ends. Thus, 3pMap detects uncharged tRNAs
326 by 3' adapter ligation to free 3' OH ends during sequencing library synthesis. We observed
327 significantly increased levels of uncharged tRNAs upon AZM treatment - one tRNA (tRNA-
328 Val) in planktonic, and twelve tRNAs in biofilm samples (tRNA-Arg, tRNA-Gln, tRNA-Gly,and
329 tRNA-Lys, tRNA-Pro, tRNA-Sec, tRNA-Thr, and tRNA-Val) (Supplementary Table S8).
330 Interestingly, the tRNA isoacceptors detected here pair with rare codons in *P. aeruginosa*
331 (Supplementary Table S8). Whether the uncharged tRNAs detected arise from reduced tRNA
332 aminoacylation, increased tRNA expression, or both in response to AZM remains to be
333 characterized (see discussion).

334 Altered premature 3'-end formation in *P. aeruginosa* genes and operons 335 in response to AZM

336 Previous work reported chronic AZM treatment impairs biofilm formation by inhibiting the
337 expression of the *lasI/lasR* and *rhlI/rhlR* QS systems [22,25,27]. QS inhibition is proposed to
338 be achieved via downregulation of the *las* and *rhl* genes [22], or downregulation of enzymes
339 responsible for QS effector synthesis [27]. The molecular mechanisms underlying AZM-
340 mediated regulation of QS regulators have not been determined. Although *lasI, lasR, rhlI,*
341 and *rhlR* were not significantly downregulated in our results, we observed significant
342 premature 3'-end peaks in *lasI* and *rhlR* upon AZM treatment (Figures 3A and Figure 3B).
343 We used the ratio of reads at intragenic peaks to full length peaks in 3' UTRs (I/FL) as a

344 metric for premature 3' end formation (Figure 1C) and evaluated relative differences in I/FL
345 in AZM-treated and untreated samples using CMH tests with a 10% FDR. To avoid false-
346 positive results, this analysis was restricted to genes with detectable intergenic and full-length
347 3'-ends in both treated and control samples (Methods). AZM-treatment led to altered I/FL in
348 550 (63.19%) and 376 (42.1%) genes in biofilm and planktonic cultures, respectively
349 (Supplementary Tables S9 and S10). Notably, AZM treatment resulted in extensive
350 premature 3' end formation in the 5'-end of *lasI* and a correspondingly large increase in I/FL
351 in biofilms (~41-fold) and in planktonic cultures (~16-fold) (Figure 4A). Similarly, an ~8-fold
352 increase in I/FL was also observed in the *rhlR* gene in AZM treated biofilms (Figure 3B). Our
353 results show that AZM disrupts full length *lasI* and *rhlR* expression by inducing premature 3'-
354 end formation within their coding sequences, possibly via premature termination,
355 transcriptional pausing or accumulation of stable nuclease products.

356 We next investigated whether the changes in premature intragenic 3'-end formation was a
357 pervasive feature of protein-coding genes differentially regulated by AZM (Figure 1C and
358 Supplementary Tables S9 and S10). In biofilms, 132 differentially expressed genes had
359 detectable intragenic and full length 3' ends in both treated and control samples, and the I/FL
360 ratios of 111 (84.0%) of these changed significantly with AZM treatment. In planktonic
361 cultures, I/FL measurements were available for 150 differentially expressed genes, and 76
362 (50.6%) changed with AZM treatment. Thus, compared to all genes, differentially expressed
363 genes in biofilm and planktonic cultures were enriched ~ 1.3-fold and ~1.2 fold for changes
364 in I/FL, respectively. Notably, the vast majority (93 of 100) of genes downregulated by AZM
365 in biofilms had increased levels of premature 3' ends compared to full length transcripts (e.g
366 Figure 3C and 3D), suggesting downregulated genes are 1.6-fold enriched for premature 3'
367 end formation (Fisher's Exact Test (FET), p = 0.001913). These include global regulators
368 *rpoS, anr*, and *relA,* as well as genes involved in biofilm formation, stress response, and
369 virulence factor genes such as *hemN* (Figure 3C, Supplementary Figure S3B), *lasB* (Figure
370 3D), *rahU, phzB1-G1* and *pelABCDEFG* [70,71,73,74,96]. The targets that exhibit no
371 evidence of enhanced premature 3' end levels in their transcript leaders, yet are still
372 significantly downregulated upon AZM treatment, may reflect expression changes in
373 upstream regulators by AZM. The *lecB*, *argR*, and *sodB* genes are notable examples
374 [25,30,77,97].

375 Changes in premature 3' end formation could also reciprocally contribute to upregulation of
376 genes in response to AZM treatment. Indeed, 18 of the 32 upregulated genes in biofilms, and

377 68 of the 118 genes upregulated in planktonic cultures exhibited corresponding decreases in
378 premature intragenic 3' end formation, an 8.1-fold enrichment in biofilms and a 2.6-fold
379 enrichment in planktonic cultures (FET $p < 7.8 \times 10^{-8}$). The most upregulated gene in AZM-
380 treated biofilms is *obgE*, a conserved GTPase involved in the stringent response and
381 persistence in *P. aeruginosa* [81,82]. Notably, *obgE* also showed the highest reduction in I/FL
382 peak ratio in response to AZM through a striking reduction in premature 3' end formation at
383 the ObgE start codon (Figure 3E and Figure 3F, Supplementary Figure S4). Thus, relief of
384 premature 3' end formation occurs at most genes upregulated by AZM and may contribute to
385 induction of the stringent response. These data suggest that premature 3' end formation
386 contributes to the gene expression response to AZM, such that increased premature 3' end
387 formation downregulates the expression of some genes, while decreased premature 3' end
388 formation upregulates the expression of others (Figure 4B).

389 **Predicting RNA regulatory elements that in *P. aeruginosa* transcript**
390 **leaders**

391 Transcription regulation by attenuators, riboswitches, RNA thermometers, sRNAs etc. can
392 result in premature 3' ends in the transcript leaders and surrounding sequences [46-49,98]**.**
393 We reasoned that transcript leaders regulated by early transcription termination, pausing,
394 and / or targeted degradation would be characterized by a high incidence of 3' end formation
395 detectable by 3pMap. To identify genes with high incidence of premature transcript termini in
396 their early termination zone (transcript leader + 40 nucleotides in the coding sequence)
397 (Figure 1B and Methods), we calculated the percentage early termini (% ET) for each gene
398 in planktonic and biofilm samples grown +/- AZM. The median %ET was < 3.0% for the tested
399 samples (Figure 1B and Supplementary Figure S3B). As riboswitch activity has been shown
400 to result in reproducible premature 3'-end termini, we used a cut-off of 30%, which is >10-
401 fold above the median %ET and sufficient to detect most riboswitches documented on Rfam
402 and predicted b Riboswitch scanner to predict genes with regulatory mechanisms causing
403 premature 3'-termini formation in their early termination zone (Supplementary Figure S4A
404 and Supplementary Table S11) [66-68]. Genes with %ET values <30% and lacking significant
405 peaks representative of reproducible 3' end termini in the transcript leaders were not
406 considered in further analysis.

407 We identified 282 protein-coding genes with more than 30% of their 3' ends in the early
408 termination zone (Supplementary Table S12). This included genes previously reported to be
409 controlled by transcription termination in *P. aeruginosa* or other bacteria, e.g. *amiE* operon

(Figure 5B and Supplementary Figure S4D-S4F), attesting to the ability of our approach to predict genes that are potentially regulated in this manner [99-102].The gene with highest early transcription termination is *rhlI,* from whose transcript leader the sRNA *rhlS* was recently reported to be derived [103]. We further utilized PASIFIC, a bioinformatic tool for predicting regulation via alternate structure formation and rho-independent termination to examine our new candidates for potential alternate structure formation and regulation by premature transcription termination [69], and ARNOLD [61] to separately predict rho-independent terminators (Supplementary Table S13). Forty-one premature termination candidate genes were predicted to have the propensity to form alternate structures and / or contain rho-independent terminators. Notably, these new candidates included several genes critical for *Pseudomonas* biology, such as the QS and virulence gene *lasR* [104](Figure 5C), DNA gyrase A (*gyrA)* - associated with fluoroquinolone-resistance currently being explored as a pharmacological target (Figure 5D) [105-107], and the cytochrome c oxidase operon (not shown). Further biochemical and functional analysis of these candidate regulatory elements could provide insights into mechanisms controlling *P. aeruginosa* gene expression. In summary, we identify hundreds of genes in *P. aeruginosa* putatively regulated by early transcription termination or nuclease action, many of which were predicted to form alternate structures.

DISCUSSION

In this study, we used 3pMap to identify RNA 3' ends in *P. aeruginosa* and to gain insights into gene regulation in response to AZM. Our study provides new insights into the role of transcriptional regulation in the *P. aeruginosa* response to AZM. Most downregulated genes, including many key transcriptional regulators and their targets - exhibit enhanced premature 3' end formation. We also found reduced transcription attenuation in some upregulated genes upon AZM treatment, most notably inducing expression of *obgE*, a central component of the stringent response. Finally, we identified over two hundred genes exhibiting high levels of premature transcript termini in or near their 5' transcript leaders. The sequences surrounding many of the premature transcript termini are predicted to form alternate structures, suggesting some may be controlled by riboregulation (Table 1). The implications of these results for understanding *P. aeruginosa* biology and therapeutic interventions are discussed below.

441 Chronic *P. aeruginosa* infections are common in CF patients, and sub-inhibitory
442 concentrations of AZM improve clinical outcomes [14,15,108]. AZM impairs biofilm formation
443 due to altered expression of QS and virulence genes [21-29]. Previous work proposed the
444 effects of AZM on QS resulted from inhibition of the synthesis of specific proteins [22,27].
445 First, AZM might disrupt the translation of an unknown protein which in turn controls the
446 transcription of autoinducer synthases *lasI and rhlI* [22]. Secondly, AZM might downregulate
447 the expression of N-acyl homoserine lactone (AHL) synthesis enzymes upstream of *lasI* and
448 *rhlI*, which in turn further dampen AHL production and inhibit QS [27]. However, because the
449 assays used in these previous studies did not differentiate between full-length and truncated
450 transcripts, neither of the resulting models consider the impact of AZM-induced translational
451 stalling on coupled mRNA transcription. We investigated the role of transcription regulation
452 on the *P. aeruginosa* response to AZM using 3pMap. AZM greatly elevated the levels of
453 premature transcripts in primary QS regulators *lasI* (in planktonic and biofilm cultures) and
454 *rhlR* (in biofilms) (Figure 3A and Figure 3B). Thus, our results suggest AZM directly impacts
455 expression of QS genes by regulating transcription or transcript stability.

456 Importantly, we found AZM induced premature transcript formation in key transcriptional
457 regulators of biofilm formation and virulence (Supplementary Table S7). Such increases in
458 premature transcript formation accompanied the downregulation of *rpoS, rpoH, vqsR* and *anr*
459 [70-72,74,75,79]. *Anr* regulates QS and virulence gene expression in low-oxygen
460 environments such as biofilms [74,75]. In QS mutants isolated from infections, *anr* plays a
461 compensatory role in virulence gene expression. The expression of *rpoS*, an alternative
462 sigma factor and a master regulator of *P. aeruginosa* stress response [70,71] was
463 downregulated by AZM in planktonic cells as well. Increased premature 3' end formation also
464 accompanied downregulation of virulence factor genes targeted by QS (*lasB, phzB-G,*
465 *pelABCD, rahU*) [25,85,86,109]. The premature 3'-ends we discovered could result from
466 altered premature termination, transcription pausing, or from nuclease activities. Taken
467 together, our results support a model in which AZM-induced premature 3' end formation
468 reduces the expression of these central transcriptional modulators (Figure 4A).

469 The effects of AZM on *P. aeruginosa* gene expression are reminiscent of previous work in
470 other bacteria, which showed ribosome-acting antibiotics can alter target gene transcription
471 by stalling translation [36,110-113]. In *E. coli,* slowing translation with sublethal
472 concentrations of chloramphenicol uncouples transcription from translation, thereby slowing
473 transcription elongation rates and/or triggering premature transcription termination [37,113].

474 Macrolide-mediated ribosome stalling is not uniformly distributed across genes but instead is
475 determined by specific sequence features of nascent polypeptides [114]. In *Staphylococcus*
476 *aureus*, AZM caused sequence-specific ribosome stalling in the middle or late stages of
477 translation [32,33]. Interestingly, AZM-specific ribosome stalling hotspots, referred to as
478 'macrolide arrest motifs' [115], were enriched in virulence-related and essential genes [114].
479 By quantifying premature transcription, we found premature transcript termini accumulate at
480 most, if not all, downregulated genes in *P. aeruginosa*. This accumulation of premature
481 transcripts likely reflects sequence-specific ribosome stalling. One interesting possibility is
482 that *P. aeruginosa* has evolved macrolide-responsive stall sequences in QS and stress
483 response genes (e.g. *rpoS* and *lasI*) to promote survival in response to macrolides produced
484 by environmental competitors [116]. Additional studies, including ribosome profiling, are
485 needed to identify translation stalling motifs in *P. aeruginosa* and further investigate antibiotic
486 induced ribosome stalling on transcription.

487 Bacterial transcription termination occurs via intrinsic and factor-dependent mechanisms
488 mediated by Rho and Mfd [44,45]. Other work has shown that sRNAs can antagonize Rho-
489 dependent termination, e.g. at the *E. coli rpoS* gene [117]. We find that roughly one-fifth of
490 reads in significant 3' end peaks correspond to predicted rho-independent or intrinsic
491 terminators, suggesting most termination in *P. aeruginosa* is factor-dependent
492 (Supplementary Table S3). AZM treatment did not considerably change the proportion of
493 reads in peaks overlapping intrinsic terminators in biofilms and planktonic cultures,
494 suggesting that factor-dependent termination could play an important role in *P. aeruginosa*
495 AZM response.

496 It is possible that some of the altered 3'-end significant peaks observed in AZM-treated
497 samples could be nuclease-degradation intermediates with stable structures. In bacteria,
498 ribosome occupancy and events occurring during translation influence the susceptibility of
499 mRNAs to ribonuclease attack [118]. Transcriptional pausing and translation-transcription
500 uncoupling are thought to increase endonucleolytic RNase cleavage [118-120]. The cleavage
501 products are quickly acted upon by 3'-exonucleases until they encounter thermodynamically
502 stable stem-loop structures. Consequently, the possibility of increased nuclease action on
503 some mature and nascent transcripts in AZM-treated samples cannot be ruled out. For
504 example, *hemN* and *rpoS* have been reported to be bound by *Hfq* in *P. aeruginosa* strain
505 PA01 in the absence of antibiotics [121]. However, we also note that low levels of antibiotics

that inhibit translation have been found to stabilize mRNAs typically associated with drug resistance in Gram-positive bacteria (e.g. *S. aureus* and *B.subtilis ermA* and *ermC* [122,123]).

An interesting observation from our study was the differential increase in tRNA 3'-end levels in response to AZM.The increased 3'-ends for tRNAs, particularly rare codon tRNAs for Arg, Lys, Pro, Gln, Gly, Sec, and Val in biofilms (Supplementary Table S7), could arise from reduced aminoacylation or an increase in tRNA gene expression. Reduced aminoacylation could cause translational stalling at rare codons, further altering the synthesis of full-length transcripts (Figure 5) [111,112]. Increased tRNA gene expression, unless accompanied by proportionate increases in aminoacylation, could dilute the pool of charged tRNA. In this case, the net effect would also be increased translational stalling at these rare codons. The influence of rare codons on translation and transcription elongation rates is well documented in *E. coli* [107], and tRNA concentrations and codon decoding times are positively correlated in many prokaryotes [108,117]. Interestingly, replacing a rare codon (AGG, frequency = 0.6 / 1000) for Arginine at the second codon position of the QS gene *rhlR* with the most frequently used codon (CGC, frequency = 48.8 / 1000) was previously shown to alleviate the inhibitory effects of AZM on virulence factor production in *P. aeruginosa* [123]**.** Our results suggest tRNAs targeting rare codons for Arg, Lys, Pro, Gln, Gly, Sec, and Val were more often uncharged after AZM treatment in biofilms. This decrease in tRNA charging could cause ribosome stalling at rare codons, altering the synthesis of full-length transcripts. Deacylated/uncharged tRNAs bind to the A-site on the ribosome, eventually triggering stringent response mechanism [125]. The stringent response leads to elevated levels alarmones such as ppGpp and ppppGpp, which are known to regulate RNA polymerase and help bacteria to survive under adverse conditions. Future work evaluating the role of tRNAs in the *P. aeruginosa* response to AZM would be beneficial.

AZM treatment caused upregulation of *obgE*, a conserved GTPase that binds ppGpp and mediates the stringent response and persistence under various stresses by increasing the dissociation of stalled 70S ribosomal units [82,126]**.** 3pMap identified a prominent 3' end significant peak in the first codon of the *obgE* ORF (Figures 3E, 3F and Supplementary Figure S4). AZM-induced upregulation of *obgE* coincided with significantly reduced levels of premature 3' end termini in the transcript leader, suggesting it may be regulated by a transcriptional attenuator. Ribosome stalling on upstream open reading frames (uORFs) in transcript leaders have been shown to relieve premature transcription termination of

538 response to the macrolide lincomycin in *L. monocytogenes* [44]. Curiously, the *obgE*
539 transcript leader contains a uORF (Figure 3F), which may play a similar role in upregulating
540 full-length transcription through attenuation. However, this attenuation-by-uORF mechanism
541 seems insufficient because the observed premature termination occurs at the *obgE* start
542 codon, which is followed by a rare codon for lysine, not in an intrinsic terminator. This
543 suggests additional regulatory factors may contribute to the switch to full length transcription
544 in the presence of azithromycin. For example, the switch to full length transcription may be
545 independent of the uORF, instead relying on Rho*,* other *trans*-acting factors or uncharged
546 tRNA. ppGpp has been shown to bind directly to *E. coli* RNA polymerase and alter its pausing
547 behavior [128], which could potentially relieve premature termination in *obgE*. Future work is
548 needed to determine the mechanisms underlying transcriptional regulation of *obgE*.

549 RNA-based regulatory strategies are gaining traction as antibacterial therapeutic targets
550 [13,52,129,130]. For example, the FMN riboswitch controls expression of flavin
551 mononucleotide synthesis operons in many bacteria. Ribocil, a small molecule that targets
552 the riboswitch by mimicking the FMN ligand, reduced bacterial growth of *E. coli* in a mouse
553 systemic infection model [129]**.** Similarly, a small molecule targeting the guanine riboswitch,
554 PC1, inhibited growth of *S. aureus* in mouse and cow infection models [130,131]. The
555 candidates we identified provide a first transcriptome-wide catalogue of candidate genes
556 regulated via mechanisms targeting transcript leaders such as premature transcription
557 termination, translation inhibition, or nuclease action in *P. aeruginosa,* which have the
558 potential to inform experimental studies to discover 'druggable RNAs'. However, due to the
559 compact nature of bacterial genomes, some of the candidate riboregulators may represent
560 termination sites from upstream genes. On the other hand, many riboswitches and
561 attenuators may still await discovery, as these elements are condition-specific and may
562 require interactions with the host immune system or other cellular stresses for their activity.
563 Additionally, some could produce novel sRNAs with regulatory roles, as was recently reported
564 for *rhlI* [103]. Thus, further studies are needed to probe the transcriptional regulation of the
565 elements identified here and to identify the full set of bona fide riboregulators in *P.*
566 *aeruginosa*.

567 Regardless of the molecular mechanisms utilized, our results reveal that the accumulation
568 of alternative 3' termini is a hallmark of the response to AZM by *P. aeruginosa* that may
569 contribute to changes in QS and virulence gene expression.We propose a model in which

570 the AZM-induced premature transcription termination, pausing, and/or nuclease action on
571 multiple central transcriptional modulators central transcriptional modulators cascades
572 through their regulatory targets (Figure 5). Furthermore, the AZM-dependent increase in
573 tRNA 3'-ends and induction of *obgE* expression suggest that AZM may trigger the stringent
574 response and persistence in *P. aeruginosa*. This implies that the efficacy of AZM as an anti-
575 virulence treatment may trade off against the induction of persister phenotypes, a
576 phenomenon warranting further study. In summary, we provide new insights into how AZM
577 treatment affects the transcriptional landscape of *P. aeruginosa*, which has important
578 implications for the development and implementation of treatments for infections.

579 ACKNOWLEDGEMENTS

580 This work was supported by the National Institute of General Medical Sciences (grant
581 R01GM121895) to C.J.M. and by the National Institute of Allergy and Infectious Diseases at
582 the National Institutes of Health (grant U01AI124302 and grant T32AI049820) and by the
583 Cystic Fibrosis Foundation Research Development Program to V.S.C. We thank Prof. Alan
584 Laederach and Jayashree Kumar, RNA Folding Bioinformatics Lab at University of North
585 Carolina, Chapel Hill for advice and discussion on alternate RNA structure prediction
586 approaches.

587 DATA AVAILABILITY

588 High-throughput sequencing data have been submitted to NCBI under Bioproject accession
589 number PRJNA639207 and GEO accession GSE173073, and will be released upon
590 publication.

591 REFERENCES

592 1. Peleg AY, Hooper DC. Hospital-acquired infections due to Gram-negative bacteria.
593 N Engl J Med. 2010;362: 1804–1813. doi:10.1056/NEJMra0904124

594 2. Driscoll JA, Brody SL, Kollef MH. The epidemiology, pathogenesis and treatment of
595 *Pseudomonas aeruginosa* infections. Drugs. 2007;67: 351–368.
596 doi:10.2165/00003495-200767030-00003

597 3. Gellatly SL, Hancock RE. *Pseudomonas aeruginosa*: new insights into pathogenesis
598 and host defenses. Pathogens Disease. 2013;67: 159–173. doi:10.1111/2049-
599 632X.12033

4. Ramirez Estrada S, Borgatta B, Rello J. *Pseudomonas aeruginosa* ventilator-associated pneumonia management. Infect Drug Resist. 2016;9: 7–18. doi:10.2147/IDR.S50669

5. Wu DC, Chan WW, Metelitsa AI, Fiorillo L, Lin AN. *Pseudomonas* skin infection: clinical features, epidemiology, and management. Am J Clin Dermatol. 2011;12: 157–169. doi:10.2165/11539770-000000000-00000

6. Markou P, Apidianakis Y. Pathogenesis of intestinal *Pseudomonas aeruginosa* infection in patients with cancer. Front Cell Infect Microbiol. 2014;3: 115. doi:10.3389/fcimb.2013.00115

7. Wagner VE, Iglewski BH. *P. aeruginosa* biofilms in CF Infection. Clin Rev Allergy Immunol. 2008;35: 124–134. doi:10.1007/s12016-008-8079-9

8. Jolivet-Gougeon A, Bonnaure-Mallet M. Biofilms as a mechanism of bacterial resistance. Drug Discov Today Technol. 2014;11: 49–56. doi:10.1016/j.ddtec.2014.02.003

9. Wei Q, Ma LZ. Biofilm matrix and its regulation in *Pseudomonas aeruginosa*. Int J Mol Sci. 2013;14: 20983–21005. doi:10.3390/ijms141020983

10. Bjarnsholt T. The role of bacterial biofilms in chronic infections. APMIS Supplementum 2013;: 1–51. doi:10.1111/apm.12099

11. Mulcahy LR, Isabella VM, Lewis K. *Pseudomonas aeruginosa* biofilms in disease. Microb Ecol. 2014;68: 1–12. doi:10.1007/s00248-013-0297-x

12. Høiby N, Krogh Johansen H, Moser C, Song Z, Ciofu O, Kharazmi A. *Pseudomonas aeruginosa* and the *in vitro* and *in vivo* biofilm mode of growth. Microbes Infect. 2001;3: 23–35. doi:10.1016/s1286-4579(00)01349-6

13. Howe RA, Spencer RC. Macrolides for the treatment of *Pseudomonas aeruginosa* infections? J Antimicrob Chemother. 1997;40: 153–155. doi:10.1093/jac/40.2.153

14. Schultz MJ. Macrolide activities beyond their antimicrobial effects: macrolides in diffuse panbronchiolitis and cystic fibrosis. J Antimicrob Chemother. 2004;54: 21–28. doi:10.1093/jac/dkh309

15. Blasi F, Bonardi D, Aliberti S, Tarsia P, Confalonieri M, Amir O, et al. Long-term azithromycin use in patients with chronic obstructive pulmonary disease and tracheostomy. Pulm Pharmacol Ther. 2010;23: 200–207. doi:10.1016/j.pupt.2009.12.002

632 16. Yousef AA, Jaffe A. The role of azithromycin in patients with cystic fibrosis. Paediatr
633 Respir Rev. 2010;11: 108–114. doi:10.1016/j.prrv.2009.12.003

634 17. Taylor SP, Sellers E, Taylor BT. Azithromycin for the prevention of COPD
635 exacerbations: The good, bad, and ugly. Am J Med. 2015;128: 1362.e1–6.
636 doi:10.1016/j.amjmed.2015.07.032

637 18. Hoffmann N, Lee B, Hentzer M, Rasmussen TB, Song Z, Johansen HK, et al.
638 Azithromycin blocks quorum sensing and alginate polymer formation and increases
639 the sensitivity to serum and stationary-growth-phase killing of *Pseudomonas*
640 *aeruginosa* and attenuates chronic *P. aeruginosa* lung infection in *Cftr(-/-)* mice.
641 Antimicrob Agents Chemother. 2007;51: 3677–3687. doi:10.1128/AAC.01011-06

642 19. Stellari F, Bergamini G, Sandri A, Donofrio G, Sorio C, Ruscitti F, et al. In vivo imaging
643 of the lung inflammatory response to *Pseudomonas aeruginosa* and its modulation
644 by azithromycin. J Transl Med. 2015;13: 251–10. doi:10.1186/s12967-015-0615-9

645 20. Molinari G, Paglia P, Schito GC. Inhibition of motility of *Pseudomonas aeruginosa*
646 and *Proteus mirabilis* by subinhibitory concentrations of azithromycin. Eur J Clin
647 Microbiol Infect Dis. 1992;11: 469–471. doi:10.1007/bf01961867

648 21. Molinari G, Guzmán CA, Pesce A, Schito GC. Inhibition of *Pseudomonas aeruginosa*
649 virulence factors by subinhibitory concentrations of azithromycin and other macrolide
650 antibiotics. J Antimicrob Chemother. 1993;31: 681–688. doi:10.1093/jac/31.5.681

651 22. Tateda K, Comte R, Pechere JC, Köhler T, Yamaguchi K, Van Delden C.
652 Azithromycin inhibits quorum sensing in *Pseudomonas aeruginosa*. Antimicrob
653 Agents Chemother. 2001;45: 1930–1933. doi:10.1128/AAC.45.6.1930-1933.2001

654 23. Favre-Bonté S, Köhler T, Van Delden C. Biofilm formation by *Pseudomonas*
655 *aeruginosa*: role of the C4-HSL cell-to-cell signal and inhibition by azithromycin. J
656 Antimicrob Chemother. 2003;52: 598–604. doi:10.1093/jac/dkg397

657 24. Gillis RJ, Iglewski BH. Azithromycin retards *Pseudomonas aeruginosa* biofilm
658 formation. J Clin Microbiol. 2004;42: 5842–5845. doi:10.1128/JCM.42.12.5842-
659 5845.2004

660 25. Nalca Y, Jänsch L, Bredenbruch F, Geffers R, Buer J, Häussler S. Quorum-sensing
661 antagonistic activities of azithromycin in *Pseudomonas aeruginosa* PAO1: a global
662 approach. Antimicrob Agents Chemother. 2006;50: 1680–1688.
663 doi:10.1128/AAC.50.5.1680-1688.2006

664 26. Skindersoe ME, Alhede M, Phipps R, Yang L, Jensen PO, Rasmussen TB, et al.
665 Effects of antibiotics on quorum sensing in *Pseudomonas aeruginosa*. Antimicrob
666 Agents Chemother. 2008;52: 3648–3663. doi:10.1128/AAC.01230-07

667 27. Kai T, Tateda K, Kimura S, Ishii Y, Ito H, Yoshida H, et al. A low concentration of
668 azithromycin inhibits the mRNA expression of N-acyl homoserine lactone synthesis
669 enzymes, upstream of *lasI* or *rhlI*, in *Pseudomonas aeruginosa*. Pulm Pharmacol
670 Ther. 2009;22: 483–486. doi:10.1016/j.pupt.2009.04.004

671 28. Imperi F, Leoni L, Visca P. Antivirulence activity of azithromycin in *Pseudomonas*
672 *aeruginosa*. Front Microbiol. 2014;5: 10. doi:10.3389/fmicb.2014.00178

673 29. Swatton JE, Davenport PW, Maunders EA, Griffin JL, Lilley KS, Welch M. Impact of
674 azithromycin on the quorum sensing-controlled proteome of *Pseudomonas*
675 *aeruginosa*. PLoS ONE. 2016;11: e0147698. doi:10.1371/journal.pone.0147698

676 30. Hassett DJ, Ma JF, Elkins JG, McDermott TR, Ochsner UA, West SE, et al. Quorum
677 sensing in *Pseudomonas aeruginosa* controls expression of catalase and superoxide
678 dismutase genes and mediates biofilm susceptibility to hydrogen peroxide. Mol
679 Microbiol. 1999;34: 1082–1093. doi:10.1046/j.1365-2958.1999.01672.x

680 31. Retsema J, Girard A, Schelkly W, Manousos M, Anderson M, Bright G, et al.
681 Spectrum and mode of action of azithromycin (CP-62,993), a new 15-membered-ring
682 macrolide with improved potency against Gram-negative organisms. Antimicrob
683 Agents Chemother. 1987;31: 1939–1947. doi:10.1128/aac.31.12.1939

684 32. Kannan K, Mankin AS. Macrolide antibiotics in the ribosome exit tunnel: species-
685 specific binding and action. Ann N Y Acad Sci. 2011;1241: 33–47. doi:10.1111/j.1749-
686 6632.2011.06315.x

687 33. Kannan K, Vázquez-Laslop N, Mankin AS. Selective protein synthesis by ribosomes
688 with a drug-obstructed exit tunnel. Cell. 2012;151: 508–520.
689 doi:10.1016/j.cell.2012.09.018

690 34. Hansen JL, Ippolito JA, Ban N, Nissen P, Moore PB, Steitz TA. The Structures of four
691 macrolide antibiotics bound to the large ribosomal subunit. Mol Cell. 2002;10: 117–
692 128. doi:10.1016/S1097-2765(02)00570-1

693 35. Sothiselvam S, Liu B, Han W, Ramu H, Klepacki D, Atkinson GC, *et al.* Macrolide
694 antibiotics allosterically predispose the ribosome for translation arrest. Proc Natl Acad
695 Sci USA. 2014;111: 9804–9809. doi:10.1073/pnas.1403586111

696 36. McGary K, Nudler E. RNA polymerase and the ribosome: the close relationship. Curr
697 Opin Microbiol. 2013;16: 112–117. doi:10.1016/j.mib.2013.01.010

698 37. Proshkin S, Rahmouni AR, Mironov A, Nudler E. Cooperation between translating
699 ribosomes and RNA polymerase in transcription elongation. Science. 2010;328: 504–
700 508. doi:10.1126/science.1184939

701 38. Fan H, Conn AB, Williams PB, Diggs S, Hahm J, Gamper HB, et al. Transcription-
702 translation coupling: direct interactions of RNA polymerase with ribosomes and
703 ribosomal subunits. Nucleic Acids Res. 2017;45: 11043–11055.
704 doi:10.1093/nar/gkx719

705 39. Conn AB, Diggs S, Tam TK, Blaha GM. Two Old Dogs, One New Trick: A review of
706 RNA polymerase and ribosome interactions during transcription-translation coupling.
707 International Journal of Molecular Sciences. 2019;20. doi:10.3390/ijms20102595

708 40. Dar D, Shamir M, Mellin JR, Koutero M, Stern-Ginossar N, Cossart P, et al. Term-seq
709 reveals abundant ribo-regulation of antibiotics resistance in bacteria. Science.
710 2016;352: aad9822–aad9822. doi:10.1126/science.aad9822

711 41. Tandonnet S, Torres TT. Traditional versus 3′ RNA-seq in a non-model species.
712 Genomics Data. 2017;11: 9–16. doi:10.1016/j.gdata.2016.11.002

713 42. Ma F, Fuqua BK, Hasin Y, Yukhtman C, Vulpe CD, Lusis AJ, et al. A comparison
714 between whole transcript and 3' RNA sequencing methods using Kapa and Lexogen
715 library preparation methods. BMC Genomics. 2019;20: 9. doi:10.1186/s12864-018-
716 5393-3

717 43. Wang X, N MPA, Jeon HJ, Lee Y, He J, Adhya S, et al. Processing generates 3' ends
718 of RNA masking transcription termination events in prokaryotes. Proc Natl Acad Sci
719 USA. 2019;116: 4440–4445. doi:10.1073/pnas.1813181116

720 44. Grylak-Mielnicka A, Bidnenko V, Bardowski J, Bidnenko E. Transcription termination
721 factor Rho: a hub linking diverse physiological processes in bacteria. Microbiology.
722 2016;162: 433–447. doi:10.1099/mic.0.000244

723 45. Roberts JW. Mechanisms of Bacterial Transcription Termination. J Mol Biol.
724 2019;431: 4030–4039. doi:10.1016/j.jmb.2019.04.003

725 46. Henkin TM, Yanofsky C. Regulation by transcription attenuation in bacteria: how RNA
726 provides instructions for transcription termination/antitermination decisions.
727 Bioessays. 2002;24: 700–707. doi:10.1002/bies.10125

728 47. Merino E, Yanofsky C. Transcription attenuation: a highly conserved regulatory
729 strategy used by bacteria. Trends in Genetics. 2005;21: 260–264.
730 doi:10.1016/j.tig.2005.03.002

731 48. Abduljalil JM. Bacterial riboswitches and RNA thermometers: Nature and
732 contributions to pathogenesis. Noncoding RNA Res. 2018;3: 54–63.
733 doi:10.1016/j.ncrna.2018.04.003

734 49. Naville M, Gautheret D. Transcription attenuation in bacteria: theme and variations.
735 Brief Funct Genomic Proteomic. 2009;8: 482–492. doi:10.1093/bfgp/elp025

736 50. Kortmann J, Narberhaus F. Bacterial RNA thermometers: molecular zippers and
737 switches. Nat Rev Microbiol. 2012;10: 255–265. doi:10.1038/nrmicro2730

738 51. Irnov I, Winkler WC. A regulatory RNA required for antitermination of biofilm and
739 capsular polysaccharide operons in Bacillales. Molecular Microbiology. 2010;76:
740 559–575. doi:10.1111/j.1365-2958.2010.07131.x

741 52. Disney MD, Dwyer BG, Childs-Disney JL. Drugging the RNA World. Cold Spring Harb
742 Perspect Biol. 2018;10: a034769. doi:10.1101/cshperspect.a034769

743 53. Nshogozabahizi JC, Aubrey KL, Ross JA, Thakor N. Applications and limitations of
744 regulatory RNA elements in synthetic biology and biotechnology. J Appl Microbiol.
745 2019;127: 968–984. doi:10.1111/jam.14270

746 54. Etzel M, Mörl M. Synthetic Riboswitches: From plug and pray toward plug and play.
747 Biochemistry. 2017;56: 1181–1198. doi:10.1021/acs.biochem.6b01218

748 55. Borges A, Simões M, Todorović TR, Filipović NR, García-Sosa AT. Cobalt Complex
749 with thiazole-based ligand as new *Pseudomonas aeruginosa* quorum quencher,
750 biofilm inhibitor and virulence attenuator. Molecules. 2018;23: 1385.
751 doi:10.3390/molecules23061385

752 56. Johansson J, Mandin P, Renzoni A, Chiaruttini C, Springer M, Cossart P. An RNA
753 thermosensor controls expression of virulence genes in *Listeria monocytogenes*. Cell.
754 2002;110: 551–561. doi:10.1016/s0092-8674(02)00905-4

755 57. Warrier I, Ram-Mohan N, Zhu Z, Hazery A, Echlin H, Rosch J, et al. The
756 Transcriptional landscape of *Streptococcus pneumoniae* TIGR4 reveals a complex
757 operon architecture and abundant riboregulation critical for growth and virulence.
758 PLoS Pathog. 2018;14: e1007461. doi:10.1371/journal.ppat.1007461

759 58. Martin M. Cutadapt removes adapter sequences from high-throughput sequencing
760 reads. EMBnetjournal. 2011;17: 10–12. doi:10.14806/ej.17.1.200

761 59. Ben Langmead, Salzberg SL. Fast gapped-read alignment with Bowtie 2. Nat
762 Methods. 2012;9: 357–359. doi:10.1038/nmeth.1923

763 60. Quinlan AR, Hall IM. BEDTools: a flexible suite of utilities for comparing genomic
764 features. Bioinformatics. 2010;26: 841–842. doi:10.1093/bioinformatics/btq033

765 61. Naville M, Ghuillot-Gaudeffroy A, Marchais A, Gautheret D. ARNold: a web tool for
766 the prediction of Rho-independent transcription terminators. RNA Biol. 2011;8: 11–
767 13. doi:10.4161/rna.8.1.13346

768 62. Freese NH, Norris DC, Loraine AE. Integrated genome browser: visual analytics
769 platform for genomics. Bioinformatics. 2016;32: 2089–2095.
770 doi:10.1093/bioinformatics/btw069

771 63. Wurtzel O, Yoder-Himes DR, Han K, Dandekar AA, Edelheit S, Greenberg EP, et al.
772 The single-nucleotide resolution transcriptome of *Pseudomonas aeruginosa* grown in
773 body temperature. PLoS Pathog. 2012;8: e1002945.
774 doi:10.1371/journal.ppat.1002945

775 64. Kent WJ, Sugnet CW, Furey TS, Roskin KM, Pringle TH, Zahler AM, et al. The human
776 genome browser at UCSC. Genome Res. 2002;12: 996–1006.
777 doi:10.1101/gr.229102

778 65. Love MI, Huber W, Anders S. Moderated estimation of fold change and dispersion for
779 RNA-seq data with DESeq2. BioMed Central; 2014;15: 1–21. doi:10.1186/s13059-
780 014-0550-8

781 66. Mukherjee S, Sengupta S. Riboswitch Scanner: an efficient pHMM-based web-server
782 to detect riboswitches in genomic sequences. Bioinformatics. 2016;32: 776–778.
783 doi:10.1093/bioinformatics/btv640

784 67. Singh P, Bandyopadhyay P, Bhattacharya S, Krishnamachari A, Sengupta S.
785 Riboswitch detection using profile hidden Markov models. BMC Bioinformatics.
786 BioMed Central; 2009;10: 325–13. doi:10.1186/1471-2105-10-325

787 68. Griffiths-Jones S, Bateman A, Marshall M, Khanna A, Eddy SR. Rfam: an RNA family
788 database. Nucleic Acids Research. 2003;31: 439–441. doi:10.1093/nar/gkg006

789 69. Millman A, Dar D, Shamir M, Sorek R. Computational prediction of regulatory,
790 premature transcription termination in bacteria. Nucleic Acids Research. 2017;45:
791 886–893. doi:10.1093/nar/gkw749

792 70. Whiteley M, Parsek MR, Greenberg EP. Regulation of quorum sensing by RpoS in
793 *Pseudomonas aeruginosa*. J Bacteriol. 2000;182: 4356–4360.
794 doi:10.1128/JB.182.15.4356-4360.2000

795 71. Schuster M, Hawkins AC, Harwood CS, Greenberg EP. The *Pseudomonas*
796 *aeruginosa* RpoS regulon and its relationship to quorum sensing. Molecular Microbiol.
797 2004;51: 973–985. doi:10.1046/j.1365-2958.2003.03886.x

72. Potvin E, Sanschagrin F, Levesque RC. Sigma factors in *Pseudomonas aeruginosa*. FEMS Microbiol Rev. 2008;32: 38–55. doi:10.1111/j.1574-6976.2007.00092.x

73. Erickson DL, Lines JL, Pesci EC, Venturi V, Storey DG. *Pseudomonas aeruginosa* relA contributes to virulence in *Drosophila melanogaster*. Infect Immun. 2004;72: 5638–5645. doi:10.1128/IAI.72.10.5638-5645.2004

74. Rompf A, Hungerer C, Hoffmann T, Lindenmeyer M, Römling U, Gross U, et al. Regulation of *Pseudomonas aeruginosa hemF* and *hemN* by the dual action of the redox response regulators Anr and Dnr. Molecular Microbiol. 1998;29: 985–997. doi:10.1046/j.1365-2958.1998.00980.x

75. Hammond JH, Dolben EF, Smith TJ, Bhuju S, Hogan DA. Links between Anr and Quorum Sensing in *Pseudomonas aeruginosa* biofilms. J Bacteriol. 2015;197: 2810–2820. doi:10.1128/JB.00182-15

76. Pérez-Martínez I, Haas D. Azithromycin inhibits expression of the GacA-dependent small RNAs RsmY and RsmZ in *Pseudomonas aeruginosa.* Antimicrob Agents Chemother. 2011;55: 3399–3405. doi:10.1128/AAC.01801-10

77. Lu C-D, Yang Z, Li W. Transcriptome analysis of the ArgR regulon in *Pseudomonas aeruginosa*. J Bacteriol. 2004;186: 3855–3861. doi:10.1128/JB.186.12.3855-3861.2004

78. Li W, Lu C-D. Regulation of carbon and ntrogen utilization by CbrAB and NtrBC two-Component systems in *Pseudomonas aeruginosa*. J Bacteriol. 2007;189: 5413–5420. doi:10.1128/JB.00432-07

79. Liang H, Deng X, Ji Q, Sun F, Shen T, He C. The *Pseudomonas aeruginosa* global regulator VqsR directly inhibits QscR to control quorum-sensing and virulence gene expression. J Bacteriol. 2012;194: 3098–3108. doi:10.1128/JB.06679-11

80. Poole K, Hay T, Gilmour C, Fruci M. The aminoglycoside resistance-promoting AmgRS envelope stress-responsive two-component system in Pseudomonas aeruginosa is zinc-activated and protects cells from zinc-promoted membrane damage. Microbiology. 2019;165: 563–571. doi:10.1099/mic.0.000787

81. Persky NS, Ferullo DJ, Cooper DL, Moore HR, Lovett ST. The ObgE/CgtA GTPase influences the stringent response to amino acid starvation in *Escherichia coli*. Molecular Microbiol. 2009;73: 253–266. doi:10.1111/j.1365-2958.2009.06767.x

82. Verstraeten N, Knapen WJ, Kint CI, Liebens V, Van den Bergh B, Dewachter L, *et al.* Obg and membrane depolarization are part of a microbial bet-hedging strategy that leads to antibiotic tolerance. Mol Cell. 2015;59: 9–21. doi:10.1016/j.molcel.2015.05.011

833 83. Lizewski SE, Schurr JR, Jackson DW, Frisk A, Carterson AJ, Schurr MJ. Identification
834 of AlgR-regulated genes in *Pseudomonas aeruginosa* by use of microarray analysis.
835 J Bacteriol. 2004;186: 5672–5684. doi:10.1128/JB.186.17.5672-5684.2004

836 84. Mavrodi DV, Bonsall RF, Delaney SM, Soule MJ, Phillips G, Thomashow LS.
837 Functional analysis of genes for biosynthesis of pyocyanin and phenazine-1-
838 carboxamide from *Pseudomonas aeruginosa* PAO1. J Bacteriol. 2001;183: 6454–
839 6465. doi:10.1128/JB.183.21.6454-6465.2001

840 85. Casilag F, Lorenz A, Krueger J, Klawonn F, Weiss S, Häussler S, et al. The LasB
841 elastase of *Pseudomonas aeruginosa* acts in concert with alkaline protease AprA to
842 prevent flagellin-mediated immune recognition. Infect Immun. 2016;84: 162–171.
843 doi:10.1128/IAI.00939-15

844 86. Rao J, Elliott MR, Leitinger N, Jensen RV, Goldberg JB, Amin AR. RahU: an inducible
845 and functionally pleiotropic protein in *Pseudomonas aeruginosa* modulates innate
846 immunity and inflammation in host cells. Cell Immunol. 2011;270: 103–113.
847 doi:10.1016/j.cellimm.2011.05.012

848 87. Belete B, Lu H, Wozniak DJ. *Pseudomonas aeruginosa* AlgR regulates type IV pilus
849 biosynthesis by activating transcription of the fimU-pilVWXY1Y2E operon. J Bacteriol.
850 2008;190: 2023–2030. doi:10.1128/JB.01623-07

851 88. Goltermann L, Good L, Bentin T. Chaperonins fight aminoglycoside-induced protein
852 misfolding and promote short-term tolerance in *Escherichia coli*. J Biol Chem.
853 2013;288: 10483–10489. doi:10.1074/jbc.M112.420380

854 89. Cardoso K, Gandra RF, Wisniewski ES, Osaku CA, Kadowaki MK, Felipach-Neto V,
855 *et al.* DnaK and GroEL are induced in response to antibiotic and heat shock in
856 *Acinetobacter baumannii*. J Med Microbiol. 2010;59: 1061–1068.
857 doi:10.1099/jmm.0.020339-0

858 90. Okuda J, Yamane S, Nagata S, Kunikata C, Suezawa C, Yasuda M. The
859 *Pseudomonas aeruginosa dnaK* gene is involved in bacterial translocation across the
860 intestinal epithelial cell barrier. Microbiology 2017;163: 1208–1216.
861 doi:10.1099/mic.0.000508

862 91. Déziel E, Gopalan S, Tampakaki AP, Lépine F, Padfield KE, Saucier M, *et al.* The
863 contribution of MvfR to *Pseudomonas aeruginosa* pathogenesis and quorum sensing
864 circuitry regulation: multiple quorum sensing-regulated genes are modulated without
865 affecting *lasRI*, *rhlRI* or the production of N-acyl-L-homoserine lactones. Mol
866 Microbiol. 2005;55: 998–1014. doi:10.1111/j.1365-2958.2004.04448.x

867 92. Colvin KM, Gordon VD, Murakami K, Borlee BR, Wozniak DJ, Wong GCL, *et al.* The
868 pel polysaccharide can serve a structural and protective role in the biofilm matrix of
869 *Pseudomonas aeruginosa*. PLoS Pathog. 2011;7: e1001264.
870 doi:10.1371/journal.ppat.1001264

871 93. Reimmann C, Beyeler M, Latifi A, Winteler H, Foglino M, Lazdunski A, et al. The
872 global activator GacA of *Pseudomonas aeruginosa* PAO positively controls the
873 production of the autoinducer N-butyryl-homoserine lactone and the formation of the
874 virulence factors pyocyanin, cyanide, and lipase. Mol Microbiol. 1997;24: 309–319.
875 doi:10.1046/j.1365-2958.1997.3291701.x

876 94. Hickman JW, Tifrea DF, Harwood CS. A chemosensory system that regulates biofilm
877 formation through modulation of cyclic diguanylate levels. Proc Natl Acad Sci USA.
878 2005;102: 14422–14427. doi:10.1073/pnas.0507170102

879 95. Choby JE, Skaar EP. Heme Synthesis and Acquisition in Bacterial Pathogens. J Mol
880 Biol. 2016;428: 3408–3428. doi:10.1016/j.jmb.2016.03.018

881 96. Tribelli PM, Lujan AM, Pardo A, Ibarra JG, Fernández Do Porto D, Smania A, *et al.*
882 Core regulon of the global anaerobic regulator Anr targets central metabolism
883 functions in *Pseudomonas* species. Sci Rep. 2019;9: 9065–13. doi:10.1038/s41598-
884 019-45541-0

885 97. da Silva DP, Matwichuk ML, Townsend DO, Reichhardt C, Lamba D, Wozniak DJ, *et*
886 *al*. The *Pseudomonas aeruginosa* lectin LecB binds to the exopolysaccharide Psl and
887 stabilizes the biofilm matrix. Nat Commun. 2019;10: 1–11. doi:10.1038/s41467-019-
888 10201-4

889 98. Winkler WC, Breaker RR. Regulation of bacterial gene expression by riboswitches.
890 Annu Rev Microbiol. 2005;59: 487–517.
891 doi:10.1146/annurev.micro.59.030804.121336

892 99. Wilson SA, Wachira SJ, Norman RA, Pearl LH, Drew RE. Transcription
893 antitermination regulation of the *Pseudomonas aeruginosa* amidase operon. The
894 EMBO Journal. 1996;15: 5907–5916. doi:10.1002/j.1460-2075.1996.tb00977.x

895 100. Ochsner UA, Reiser J. Autoinducer-mediated regulation of rhamnolipid biosurfactant
896 synthesis in *Pseudomonas aeruginosa*. Proc Natl Acad Sci USA. 1995;92: 6424–
897 6428. doi:10.1073/pnas.92.14.6424

898 101. Fu Y, Deiorio-Haggar K, Anthony J, Meyer MM. Most RNAs regulating ribosomal
899 protein biosynthesis in *Escherichia coli* are narrowly distributed to
900 Gammaproteobacteria. Nucleic Acids Res. 2013;41: 3491–3503.
901 doi:10.1093/nar/gkt055

902 102. Olekhnovich I, Gussin GN. Effects of mutations in the *Pseudomonas putida miaA*
903 gene: regulation of the *trpE* and *trpGDC* operons in *P. putida* by attenuation. J
904 Bacteriol. 2001;183: 3256–3260. doi:10.1128/JB.183.10.3256-3260.2001

905 103. Thomason MK, Voichek M, Dar D, Addis V, Fitzgerald D, Gottesman S, *et al.* A *rhlI 5'*
906 UTR-derived sRNA regulates RhlR-dependent quorum sensing in *Pseudomonas*
907 *aeruginosa*. mBio. 2019;10: 43. doi:10.1128/mBio.02253-19

908 104. Gilbert KB, Kim TH, Gupta R, Greenberg EP, Schuster M. Global position analysis of
909 the *Pseudomonas aeruginosa* quorum-sensing transcription factor LasR. Mol
910 Microbiol. 2009;73: 1072–1085. doi:10.1111/j.1365-2958.2009.06832.x

911 105. Mouneimné H, Robert J, Jarlier V, Cambau E. Type II topoisomerase mutations in
912 ciprofloxacin-resistant strains of *Pseudomonas aeruginosa.* Antimicrob Agents
913 Chemother. 1999;43: 62–66.

914 106. Dages S, Dages K, Zhi X, Leng F. Inhibition of the *gyrA* promoter by transcription-
915 coupled DNA supercoiling in *Escherichia coli*. Sci Rep. 2018;8: 1–9.
916 doi:10.1038/s41598-018-33089-4

917 107. Kaguni JM. The macromolecular machines that duplicate the *Escherichia coli*
918 chromosome as targets for drug discovery. Antibiotics(Basel). 2018;7: 23.
919 doi:10.3390/antibiotics7010023

920 108. Howe RA, Spencer RC. Macrolides for the treatment of *Pseudomonas aeruginosa*
921 infections? J Antimicrob Chemother. 1997;40: 153–155. doi:10.1093/jac/40.2.153

922 109. Friedman L, Kolter R. Genes involved in matrix formation in *Pseudomonas*
923 *aeruginosa* PA14 biofilms. Mol Microbiol. 2004;51: 675–690. doi:10.1046/j.1365-
924 2958.2003.03877.x

925 110. Dana A, Tuller T. The effect of tRNA levels on decoding times of mRNA codons.
926 Nucleic Acids Res. 2014;42: 9171–9181. doi:10.1093/nar/gku646

927 111. Buskirk AR, Green R. Ribosome pausing, arrest and rescue in bacteria and
928 eukaryotes. Philos Trans R Soc Lond, B, 2017;372: 20160183.
929 doi:10.1098/rstb.2016.0183

930 112. Rodnina MV. Translation in prokaryotes. Cold Spring Harb Perspect Biol. 2018;10:
931 a032664. doi:10.1101/cshperspect.a032664

932 113. Zhu M, Mori M, Hwa T, Dai X. Disruption of transcription–translation coordination in
933 *Escherichia coli* leads to premature transcriptional termination. Nat Microbiol. 2019;4:
934 2347–2356. doi:10.1038/s41564-019-0543-1

935 114. Davis AR, Gohara DW, Yap M-NF. Sequence selectivity of macrolide-induced
936 translational attenuation. Proc Natl Acad Sci USA. 2014;111: 15379–15384.
937 doi:10.1073/pnas.1410356111

938 115. Vázquez-Laslop N, Mankin AS. How macrolide antibiotics work. Trends Biochem Sci.
939 2018;43: 668–684. doi:10.1016/j.tibs.2018.06.011

940 116. Linares JF, Gustafsson I, Baquero F, Martinez JL. Antibiotics as intermicrobial
941 signaling agents instead of weapons. Proc Natl Acad Sci USA. 2006;103: 19484–
942 19489. doi:10.1073/pnas.0608949103

943 117. Sedlyarova N, Shamovsky I, Bharati BK, Epshtein V, Chen J, Gottesman S, et al.
944 sRNA-mediated control of transcription termination in *E. coli*. Cell. 2016;167: 111–
945 121.e13. doi:10.1016/j.cell.2016.09.004

946 118. Deana A, Belasco JG. Lost in translation: the influence of ribosomes on bacterial
947 mRNA decay. Genes Dev. 2005;19: 2526–2533. doi:10.1101/gad.1348805

948 119. Iost I, Dreyfus M. The stability of *Escherichia coli lacZ* mRNA depends upon the
949 simultaneity of its synthesis and translation. The EMBO J. 1995;14: 3252–3261.
950 doi:10.1002/j.1460-2075.1995.tb07328.x

951 120. Sunohara T, Jojima K, Tagami H, Inada T, Aiba H. Ribosome stalling during
952 translation elongation induces cleavage of mRNA being translated in *Escherichia coli*.
953 J Biol Chem. 2004;279: 15368–15375. doi:10.1074/jbc.M312805200

954 121. Kambara TK, Ramsey KM, Dove SL. Pervasive targeting of nascent transcripts by
955 Hfq. Cell Rep. 2018;23: 1543–1552. doi:10.1016/j.celrep.2018.03.134

956 122. Sandler P, Weisblum B. Erythromycin-induced stabilization of *ermA* messenger RNA
957 in *Staphylococcus aureus* and *Bacillus subtilis*. J Mol Biol. 1988;203: 905–915.
958 doi:10.1016/0022-2836(88)90116-7

959 123. Bechhofer DH, Zen KH. Mechanism of erythromycin-induced *ermC* mRNA stability in
960 *Bacillus subtilis*. J Bacteriol. 1989;171: 5803–5811. doi:10.1128/jb.171.11.5803-
961 5811.1989

962 124. Gödeke J, Pustelny C, Häussler S. Recycling of peptidyl-tRNAs by peptidyl-tRNA
963 hydrolase counteracts azithromycin-mediated effects on *Pseudomonas aeruginosa*.
964 Antimicrob Agents Chemother. 2013;57: 1617–1624. doi:10.1128/AAC.02582-12

965 125. Raina M, Ibba M. tRNAs as regulators of biological processes. Front Genet. Frontiers;
966 2014;5: 22901. doi:10.3389/fgene.2014.00171

967 126. Feng B, Mandava CS, Guo Q, Wang J, Cao W, Li N, et al. Structural and functional
968 insights into the mode of action of a universally conserved Obg GTPase. Petsko GA,
969 editor. PLoS Biol. 2014;12: e1001866. doi:10.1371/journal.pbio.1001866

970 127. Larson MH, Mooney RA, Peters JM, Windgassen T, Nayak D, Gross CA, et al. A
971 pause sequence enriched at translation start sites drives transcription dynamics *in*
972 *vivo*. Science. 2014;344: 1042–1047. doi:10.1126/science.1251871

973 128. Gourse RL, Chen AY, Gopalkrishnan S, Sanchez-Vazquez P, Myers A, Ross W.
974 Transcriptional responses to ppGpp and DksA. Annu Rev Microbiol. 2018.
975 doi:10.1146/annurev-micro-090817-062444

976 129. Dersch P, Khan MA, Mühlen S, Görke B. Roles of regulatory RNAs for antibiotic
977 resistance in bacteria and their potential value as novel drug targets. Front Microbiol.
978 2017;8: 803. doi:10.3389/fmicb.2017.00803

979 130. Mulhbacher J, Brouillette E, Allard M, Fortier L-C, Malouin F, Lafontaine DA. Novel
980 riboswitch ligand analogs as selective inhibitors of guanine-related metabolic
981 pathways. PLoS Pathog. 2010;6: e1000865. doi:10.1371/journal.ppat.1000865

982 131. Ster C, Allard M, Boulanger S, Lamontagne Boulet M, Mulhbacher J, Lafontaine DA,
983 et al. Experimental treatment of *Staphylococcus aureus* bovine intramammary
984 infection using a guanine riboswitch ligand analog. J Dairy Sci. 2013;96: 1000–1008.
985 doi:10.3168/jds.2012-5890

986

Figure 1

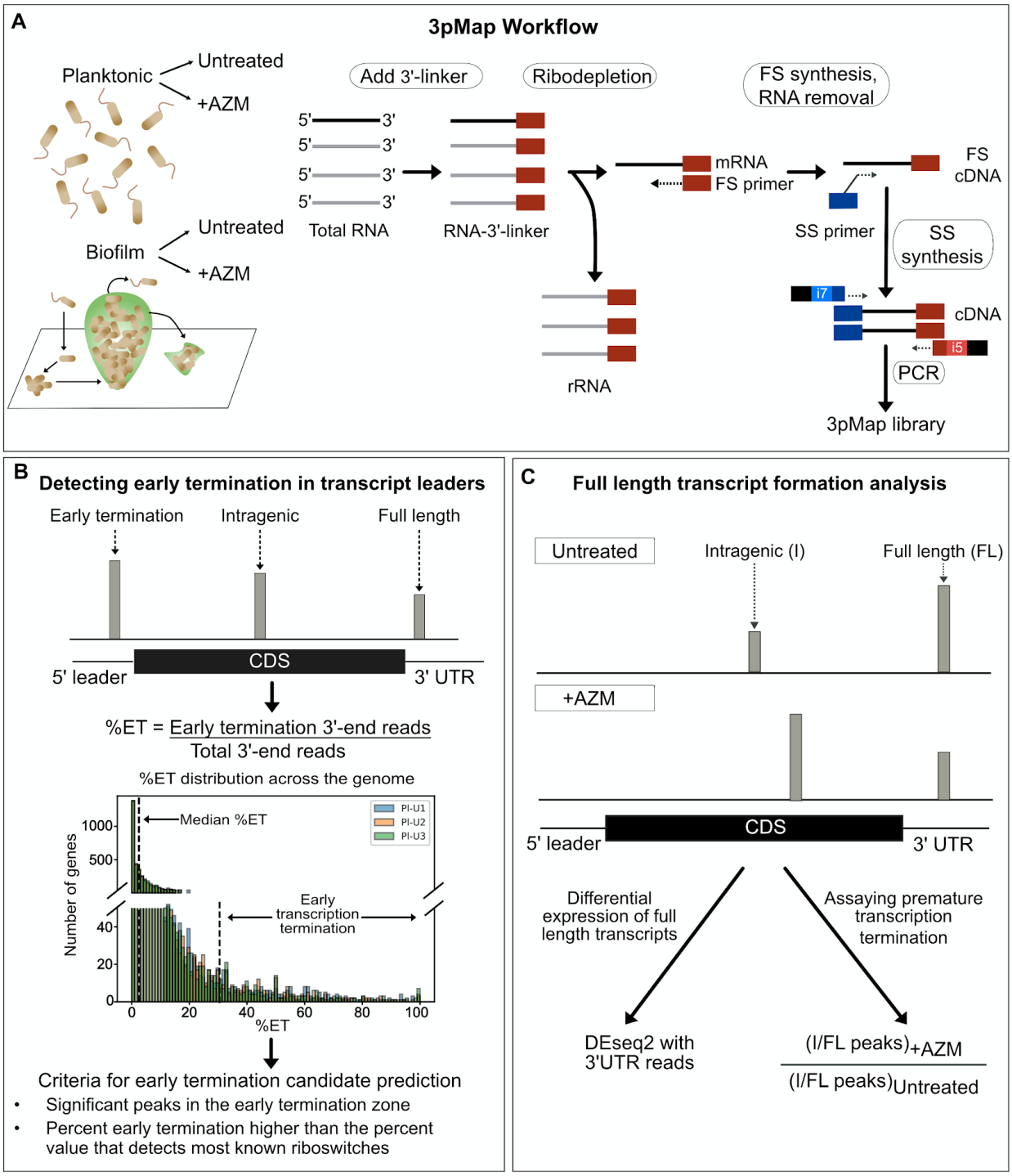

Figure 1. 3pMap workflow and data analysis. (A) 3pMap library synthesis. A 3' adapter is ligated to total RNA, followed by rRNA depletion. The cDNA is generated by reverse transcription with oligos containing sequences complementary to the adapter (first strand, FS) and to random priming sites (second strand, SS). The cDNA libraries are PCR amplified to generate Illumina sequencing libraries. **(B)** Predicting RNA regulatory elements in transcript leader neighborhood. 3' end reads are assigned to genes /operons and categorized as early termini (transcript leader + 40 nucleotides) (ET), intragenic (I), and 3'UTR or full

995 length (FL) reads. Genes with significant 3' end peaks in the ET zone and %ET >30 are
996 considered outlier candidates. **(C)** Assaying changes in full length transcript synthesis. 3' end
997 reads and peaks were categorized as intragenic (I) and full length (FL) depending on their
998 locations. Differential changes in gene expression were measured using DEseq2 of all 3' end
999 reads (see Methods). Relative changes in premature 3' end formation were measured by
1000 comparing the I/FL peaks in AZM-treated vs. untreated samples.

1001

1002

1003

1004

1005

1006

1007

1008

1009

1010

1011

Figure 2

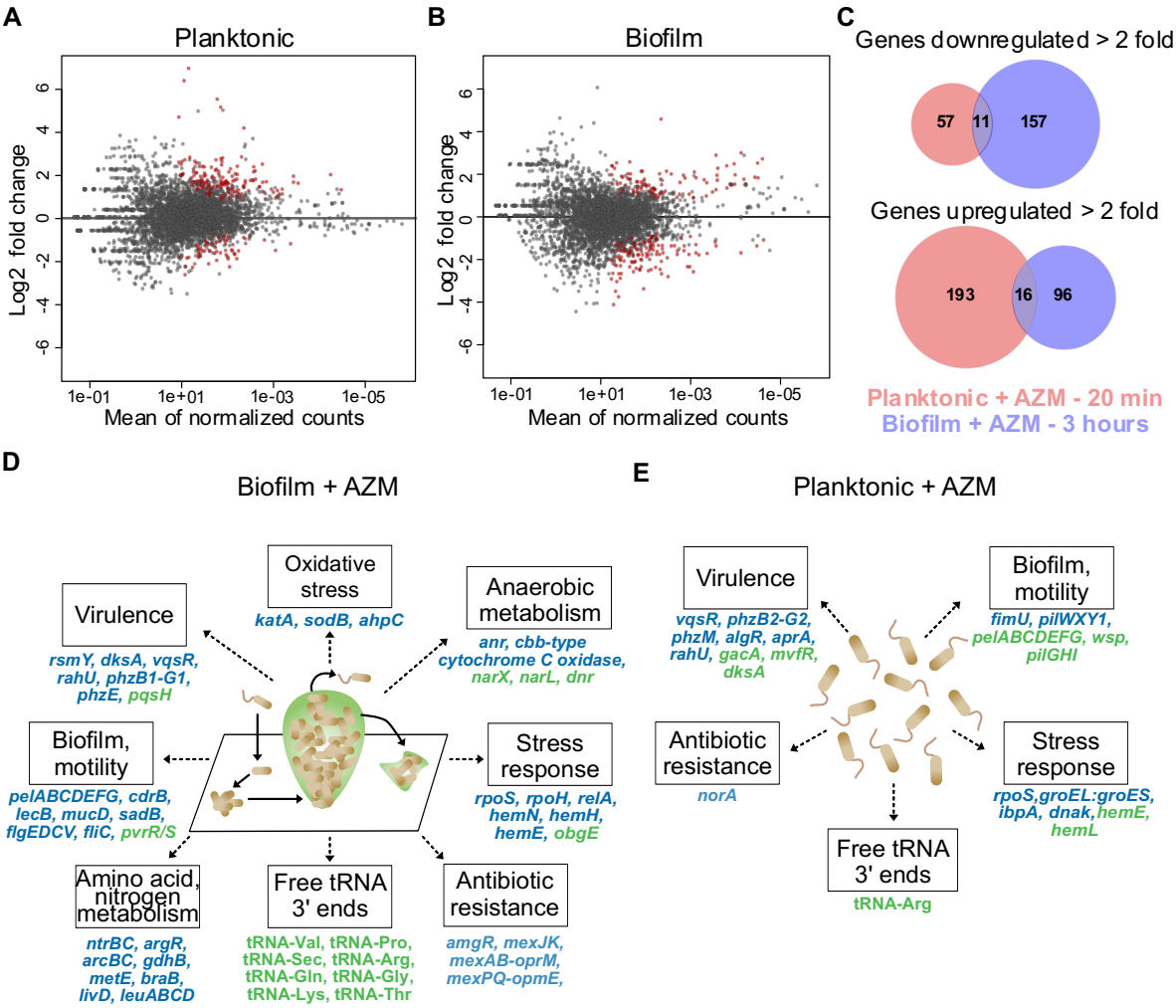

Figure 2. AZM alters full length transcript synthesis of *P. aeruginosa* genes. (A and B) Scatter plot of DEseq2 analysis of expression changes in PA14 planktonic cultures and biofilms treated with AZM. Red dots indicate DEseq changes at 10% FDR. (C) Genes showing >2 fold down (top) or up (bottom) differential regulation upon AZM treatment. AZM induced regulation of planktonic and biofilm genes, indicated in red and blue, respectively, show little overlap. Key PA14 genes regulated by AZM in biofilm (D) cultures and planktonic (E) cultures. Downregulated genes are colored blue, whereas upregulated genes are colored green. Many of these genes have pleiotropic functions, thus impact additional cell processes beyond the primary category in which they are shown here.

Figure 3

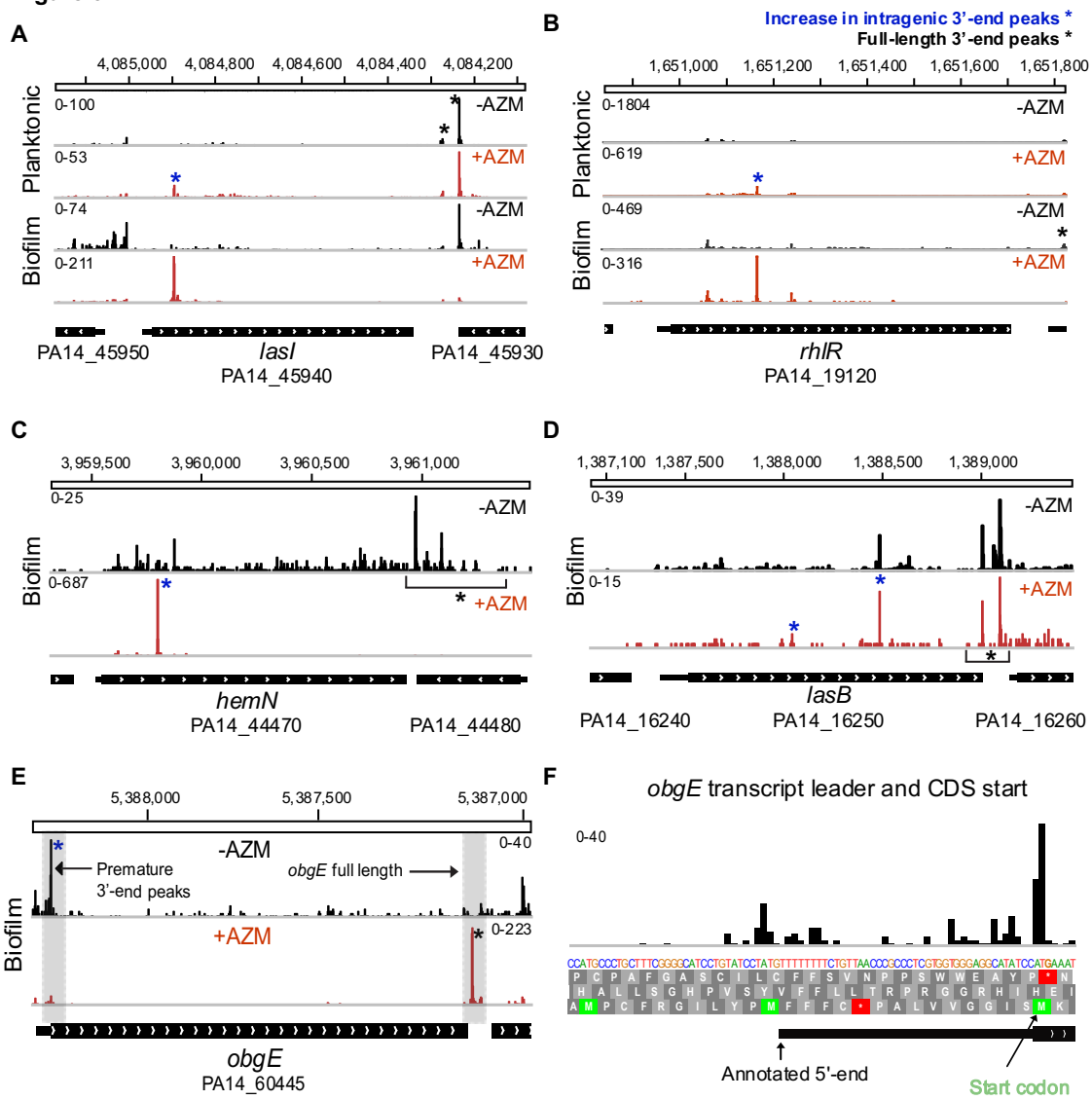

Figure 3. AZM alters intragenic 3' end peak formation in PA14 genes. **(A and B)** AZM dependent increase in intragenic premature 3' end peaks in *lasI* and *rhlR* genes. IGV views of *lasI* and *rhlR* in control (-AZM) and AZM treated (+AZM) treated samples from planktonic and biofilm cultures are shown. Intragenic peaks whose relative levels are altered by AZM are indicated with blue asterisks. The *lasI* gene in planktonic cultures and biofilm showed ~16 fold and ~41 fold increase in I/FL peak ratio upon AZM treatment, respectively. AZM treatment resulted in an ~8 fold increase in I/FL peaks for *rhlR* in biofilms. The peak is not prominent in planktonic cultures. **(C)** IGV view of the *hemN* gene downregulated by AZM (DEseq2 $\log_2$fold change = -1.2) shows a 60 fold increase in I/FL peak ratio. The effect is less pronounced in planktonic cells **(D)** IGV view of *lasB* downregulated by AZM (DEseq2 change = ~1.95) shows moderate increase in I/FL ratio (1.74 fold) in the presence of AZM. **(E)** 23 fold upregulation of *obgE* (is accompanied by a 42-fold reduction in transcription attenuation in its transcript leader. **(F)** A closer view of the transcript leader and CDS start shows termination before the rare codon for Lys at the *obgE* start codon.

1040 **Figure 4**

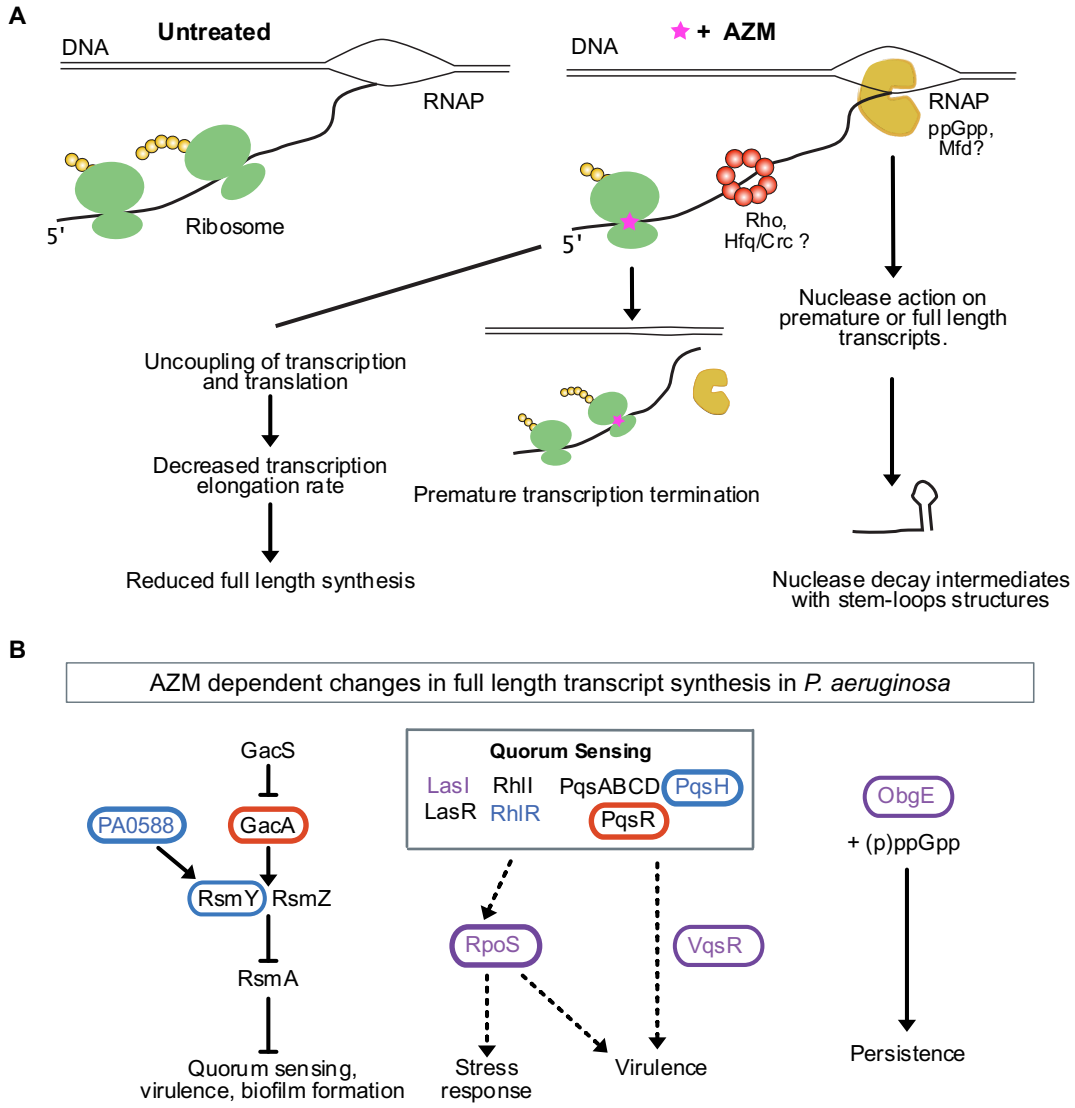

1041

1042 **Figure 4. Model of *P. aeruginosa* response to azithromycin**. **(A)** Altered premature 3'-end
1043 formation is observed in up and down-regulated genes/operons of *P. aeruginosa* in response
1044 to AZM. AZM induces changes in premature transcription termination, transcription pausing
1045 and/or transcription elongation rate, due to transcription-translation uncoupling or altered
1046 RNA polymerase pausing in response to ppGpp, thereby resulting in gene expression
1047 changes. Alternatively, nuclease action on premature and full-length transcripts could
1048 contribute to gene expression changes in response to AZM. Different molecular mediators of
1049 transcriptional control that could affect transcriptional changes are indicated – Rho and Mfd
1050 (transcription termination), ppGpp (RNAP pausing), and Hfq (sRNA action and nuclease
1051 recruitment). **(B)** Impact of AZM on gene expression of key *P. aeruginosa* regulators. Network
1052 diagram depicts several genes found to be differentially regulated and exhibit premature
1053 transcription termination within the GacS/GacA signal transduction system, quorum sensing
1054 systems, and stringent response regulators. These genes, and their regulons, have been
1055 shown to be highly interconnected, therefore only a subsection of interactions are shown
1056 here. Oval outlines indicate that a gene was differentially expressed upon AZM treatment as
1057 detected by DESeq2. Significant hits for altered relative I/FL ratio upon AZM treatment is
1058 shown by color of the text. Genes with altered expression or early transcription termination

1059 in biofilms are indicated in blue, in planktonic culture in red, and in both conditions in purple.
1060 The nature of the expression changes is indicated in Figure 3D.

1061

1062 **Figure 5**

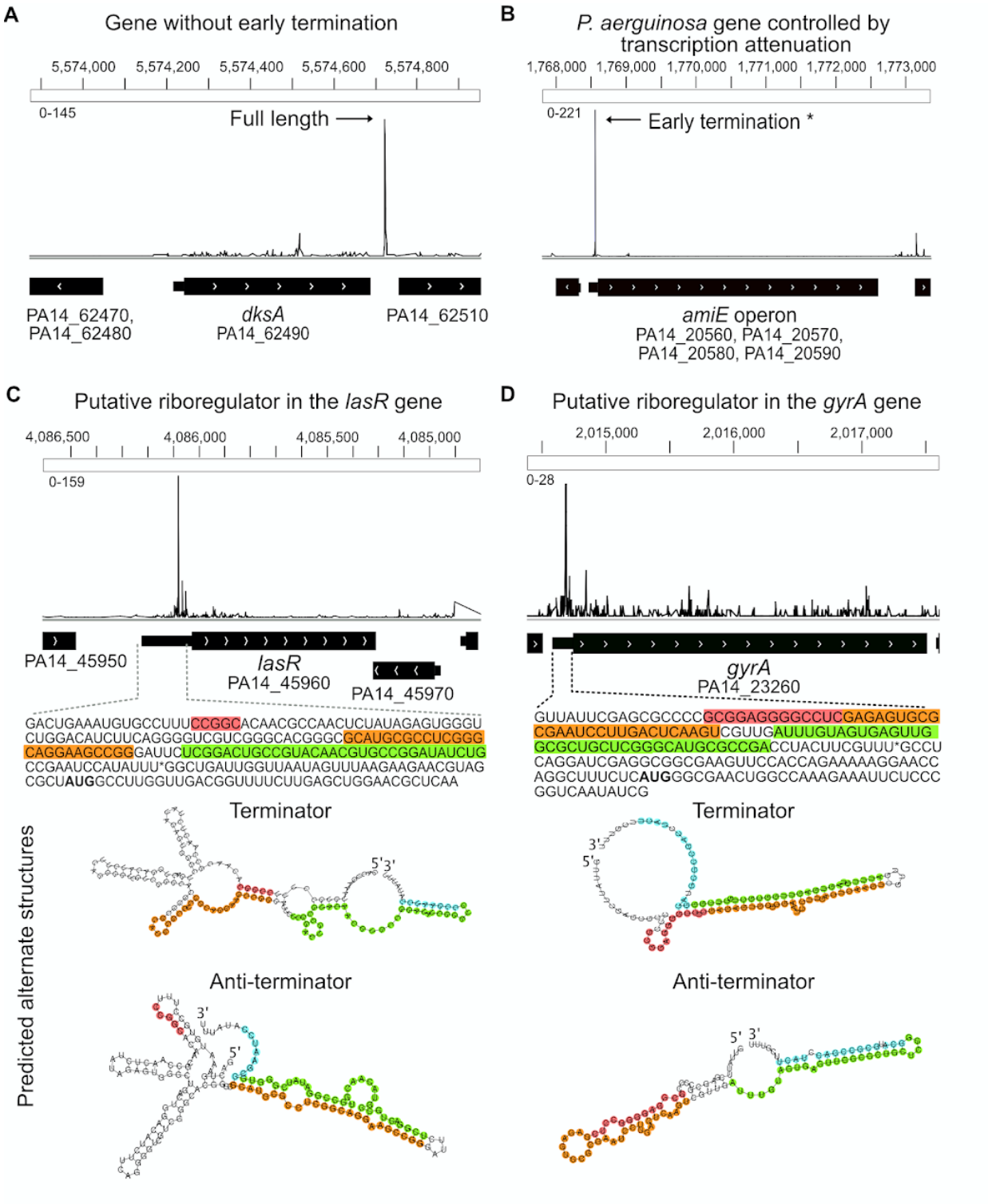

1063

1064 **Figure 5. Predicting genes regulated by premature 3' end formation in transcript**
1065 **leaders**. IGV views show strand-specific 3' end counts. (A) Example of a gene (*dksA*
1066 PA14_62490) not predicted to be regulated by premature transcription termination in its
1067 transcript leader. The major 3' end peak is in the 3' UTR. (B) IGV view of early termination in
1068 the *amiE* operon, known to be regulated by transcription attenuation, shows major 3' end
1069 peak in transcript leader. (C) IGV view of *lasR* shows premature 3' end peaks in its transcript
1070 leader. The sequence of the *lasR* early termination region and predicted alternate secondary

1071 structures in the transcript leader are shown below. The asterisk denotes a premature 3' end
1072 peak. Alternate structures with potential to effect early termination (terminator and
1073 transcriptional read-through (anti-terminator was predicted with PASIFIC [68] using the
1074 sequence upstream of the asterisk (corresponding to a 3' end significant peak) as the input.
1075 (D) IGV view of DNA gyrase A (*gyrA)* shows premature 3' ends in its transcript leader. The
1076 sequence of *gyrA* transcript leader and 40 nt in the CDS and the alternate structures
1077 predicted by PASIFIC are shown below, as in C.

1078

1079 **SUPPLEMENTARY FIGURES**

1080 **Supplementary Figure S1**.

1081

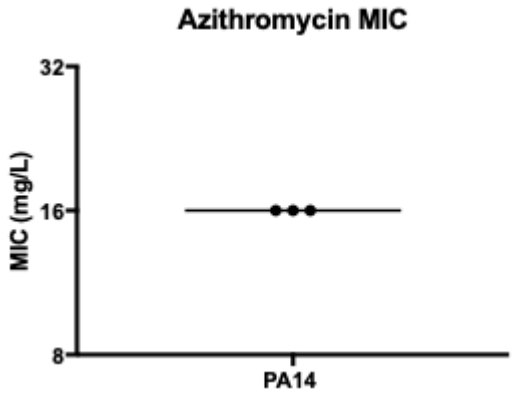

1082

1083

1084 **Supplementary Figure S1**. The **Minimum Inhibitory Concentration (MIC)**of AZM was
1085 determined by broth microdilution according to CLSI guidelines [1]. Three replicate assays
1086 were performed. Briefly, twofold microdilutions of Azithromycin dihydrate (Fisher J66740) in
1087 Mueller Hinton Broth were inoculated with $5x10^5$ CFU/mL PA14 in a 96 well plate. After 16-
1088 20 hours of incubation at 37ºC, MIC was determined to be the lowest concentration of
1089 antibiotic at which no visible growth was observed.

1090

Supplementary Figure S2

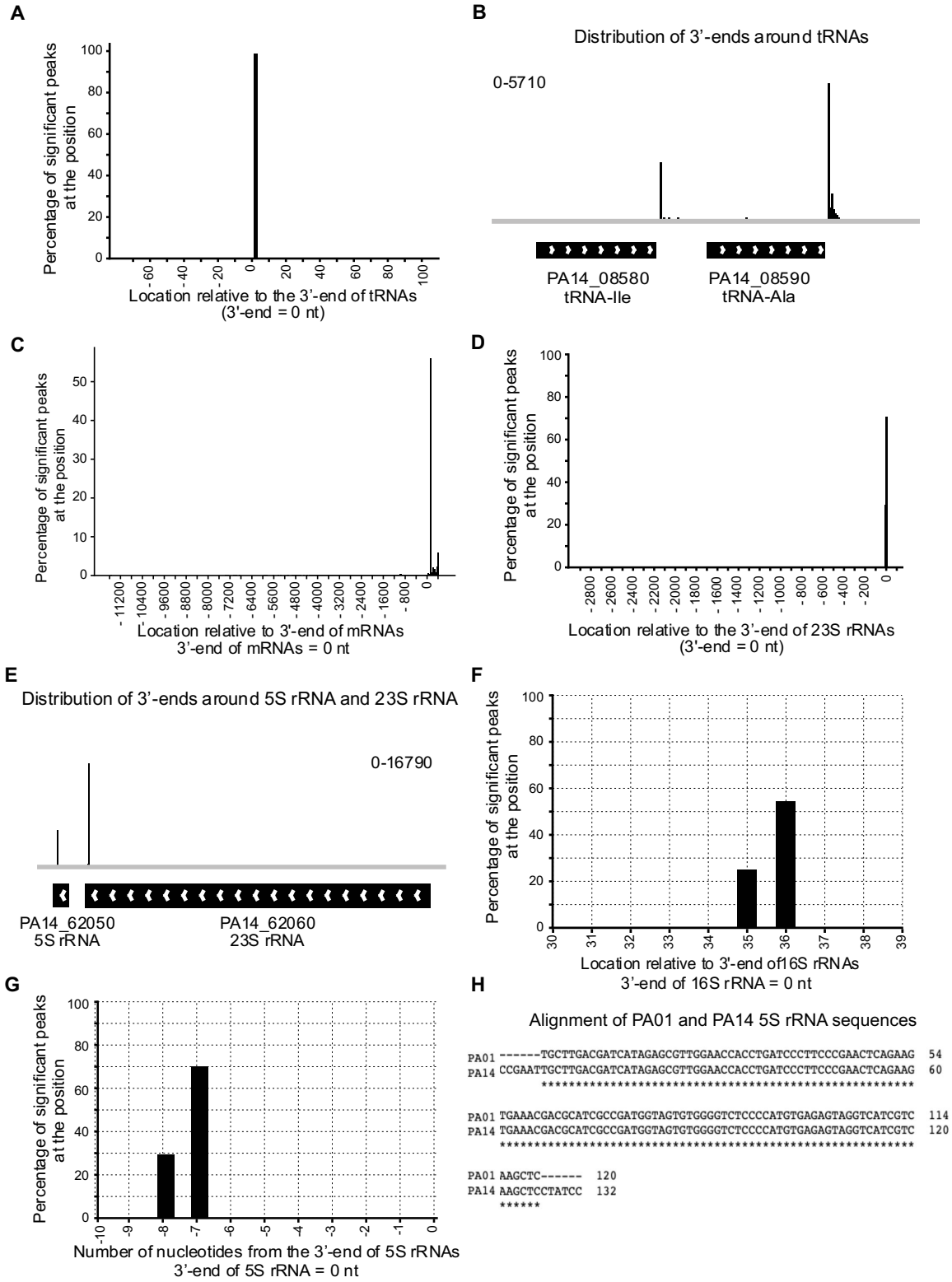

Supplementary Figure S2. Genome-wide mapping of RNA 3' ends in untreated planktonic cultures of PA14 using 3pMap. **(A).** Location of 3pMap reads with respect to the 3' end of tRNAs (RNA end = 0 nucleotide). 98.78% of the significant peaks within or downstream of tRNAs are located within 3 nucleotides from the annotated RNA ends. **(B)** Genome browser

view of distribution of 3' ends around two tRNA genes. Number of 3' end reads corresponding to each sample are denoted on the top of the sample tracks. **(C)** Location of 3pMap reads with respect to the 3' end of CDSs. RNA 3' end = 0 nucleotide. 88.4% of significant peaks associated with mRNAs were located in intergenic regions, with <12% located within coding sequences. **(D)** Location of 3pMap reads with respect to the 3' end of 23S ribosomal RNAs. 99.8% of the significant peaks within or downstream of 23SrRNA genes are located within 3 nucleotides of the annotated RNA ends. **(E)** Genome browser view of the distribution of 3' ends around representative 23S rRNA and 5S rRNA genes. **(F)** Extended 16S rRNAs in *Pseudomonas aeruginosa.* 80.54% of the detected 16S rRNAs (<10,000 reads in three replicates) had RNA 3' ends in +35 and +36 nucleotides downstream of their annotated RNA 3' ends. A recent study reported extended anti-Shine Dalgarno motifs in 16S rRNA in other bacteria, although they failed to identify such a motif in *P. aeruginosa* [2]. The major peak +35/36 downstream of 16S rRNA could represent extended anti-Shine Dalgarno motifs in *P. aeruginosa* 16S rRNA, capable of providing additional specificity or transcript preference for Shine Dalgarno motifs on mRNA, or unprocessed pre-16S rRNAs [2,3]. **(G)** 99.9% of RNA 3' end significant peaks associated with 5S rRNAs were located -8 or -7 nucleotides upstream of their annotated RNA ends. **(H)** Alignment of 5S rRNA sequences from PA01 and PA14 genome annotations using Clustal Omega (www.ebi.ac.uk). The prokaryotic 5S rRNA sequence is well conserved and 120 nucleotides long, including in the PAO1 strain (Pseudomonas genome database). We aligned the 5S rRNA sequences from PAO1 and our PA14 using Clustal Omega (www.ebi.ac.uk), and found that the 3' end identified by 3pMap is identical to PAO1. The 3' end identified by 3pMap matches with the annotated PA01 5S rRNA 3' end.

L120 **Supplementary Figure S3**

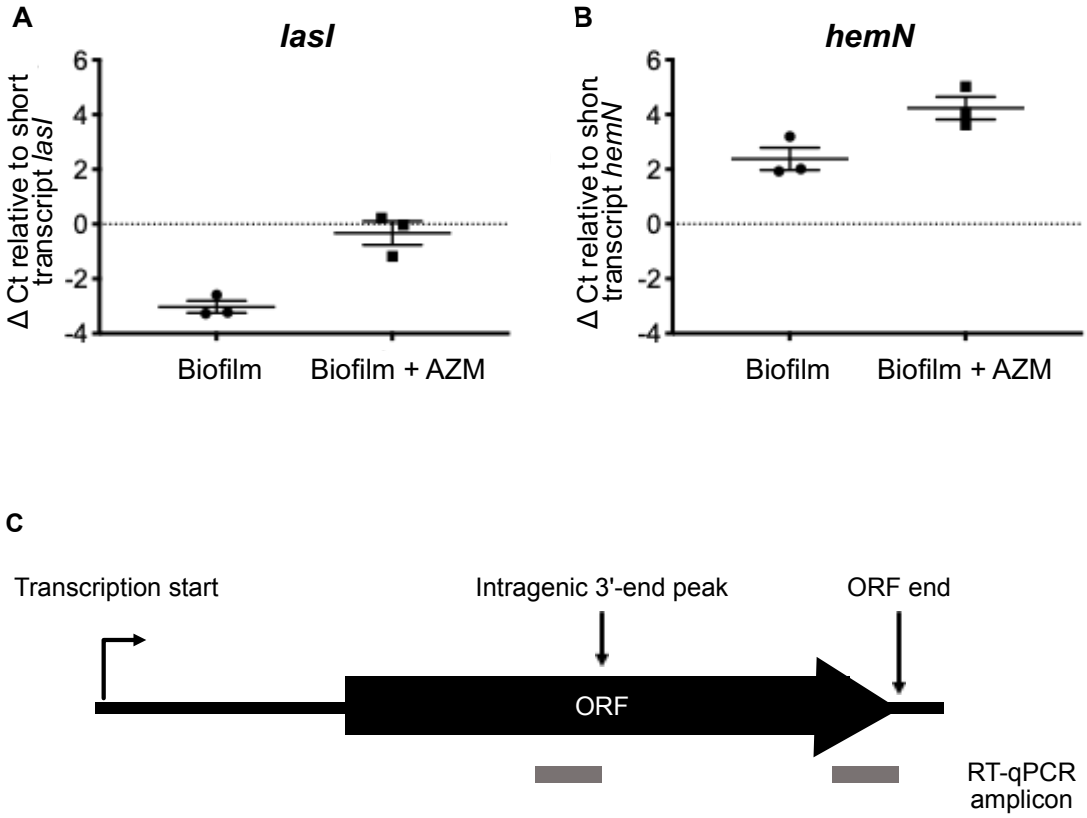

L121

L122

L123 **Supplementary Figure S3.** Changes in intragenic to full-length transcript ratios of *lasI* and
L124 *hemN.* Total RNA was phenol-chloroform extracted from biofilm samples and treated with 1
L125 unit of RQ1 RNase-Free DNase (Promega M6101) according to manufacturer's protocol to
L126 remove any residual genomic DNA. DNase-treated RNA was reverse transcribed using a 2
L127 μM pooled mixture of reverse primers for the target genes of interest (Supplementary Table
L128 S14) and Superscript IV Reverse Transcriptase (Thermofisher Scientific 18090010). The
L129 reverse transcription reaction for intragenic and full-length transcripts were performed for 20
L130 minutes at 55ºC. cDNA was amplified with the corresponding primer pairs (Supplementary
L131 Table S14) for targets of interest and Sybr Green PowerUp Master Mix (Thermofisher
L132 Scientific A25741) according to the manufacturer's protocol on Applied Biosystems StepOne
L133 Plus Real-Time PCR system. For each condition, three biological replicates were tested, with
L134 three technical replicates for each.

L135

L136

Supplementary Figure S4

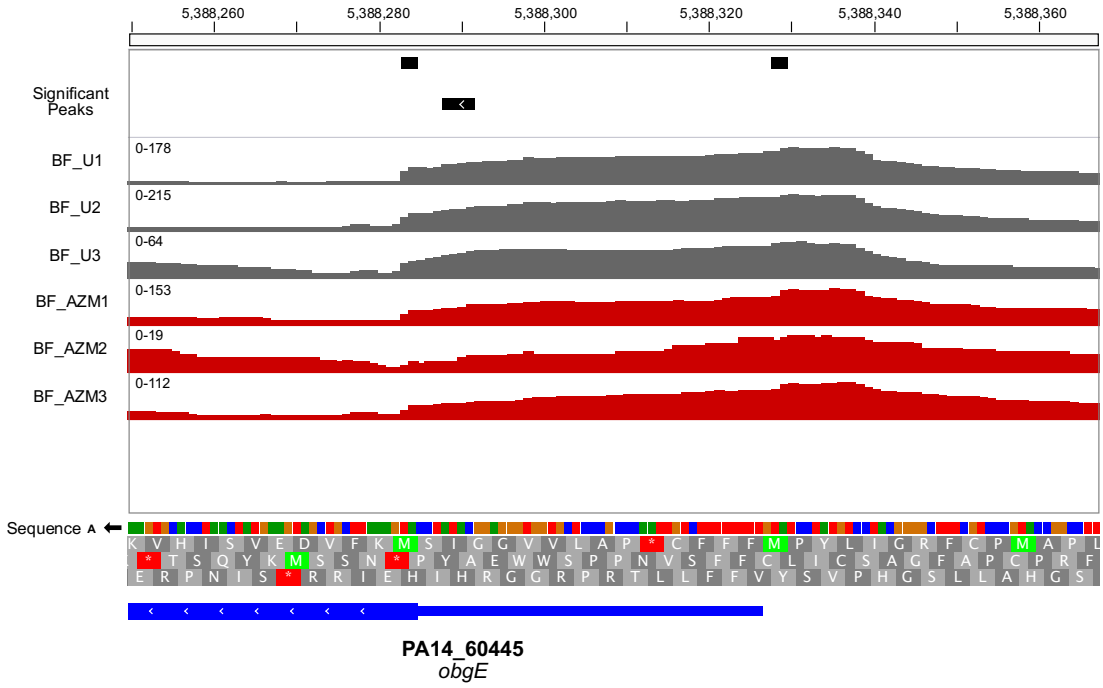

Supplementary Figure S4. Full coverage strand-specific 3pMap reads for *obgE* transcript leader. Tracks for all three replicates of biofilm treated (AZM) and untreated (U) samples are shown. The numbers on the scale depict original, non-normalized read counts. Both AUG methionines of the potential uORF, though outside the annotated transcript leader from Wurtzel et al., are covered by transcribed RNA in vivo. Note the strong accumulation of 3' ends at the *obgE* start codon, which appears as a "cliff" before coverage drops (compare to Figure 3).

Supplementary Figure S5

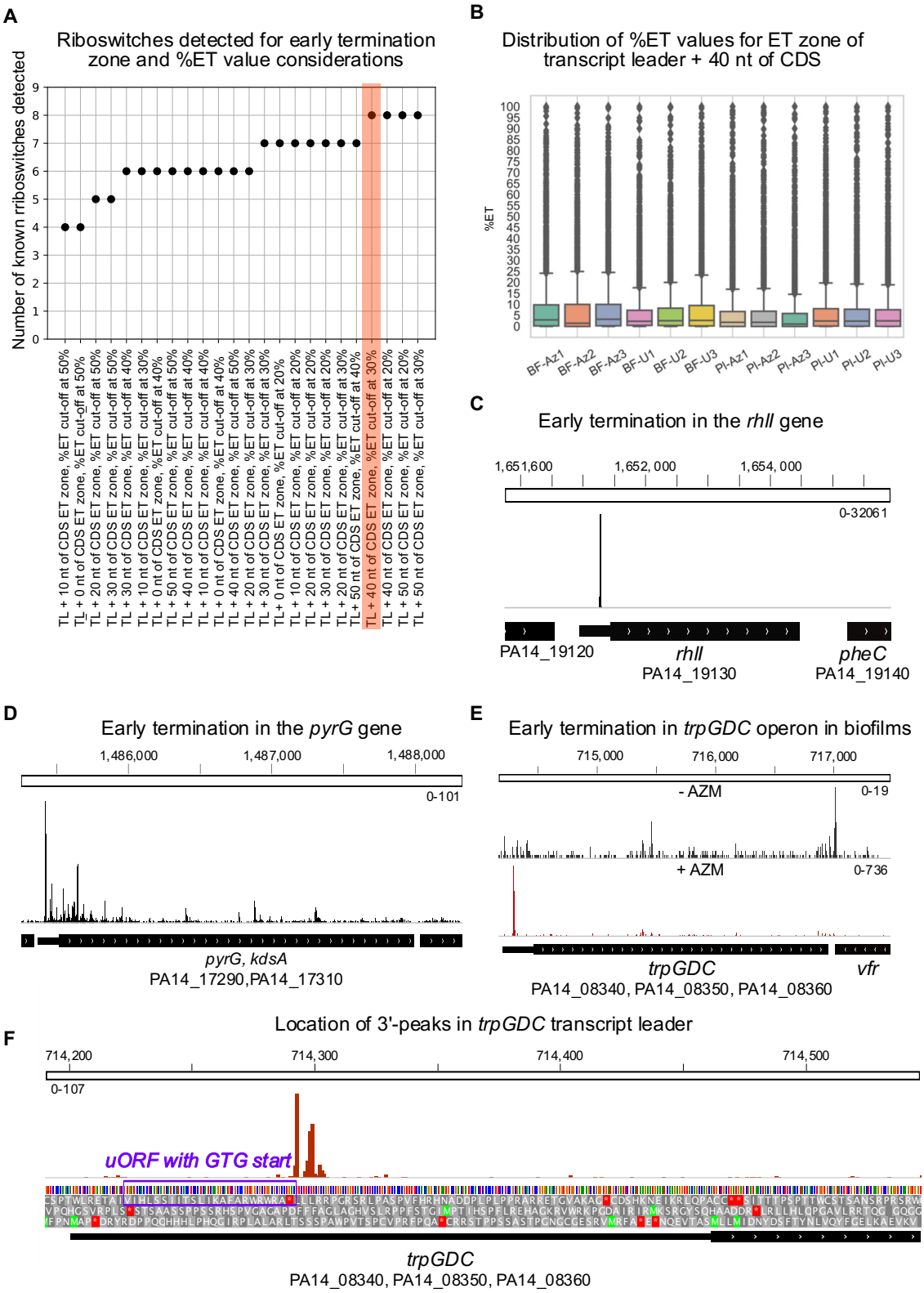

Supplementary Figure S5. Early Termination in PA14 transcript leaders. (A) Determining the early termination zone. Number of known riboswitches reported on Rfam detected for each ET zone and %ET cut off considerations. The lowest ET zone consideration

of transcript leader + 40 nt in CDS and the highest cut-off value of 30% detected 8/11 riboswitches reported on Rfam, and was therefore used for predicting gputative riboregulators. **(B)** Box Whisker plot showing the distribution of %ET values in samples using ET zone transcript leader + 40 nt of CDS. **(C)** Early transcription termination in the *rhlI* gene detected by 3pMap [4]. Genome browser images show strand-specific tracks for the strand same as the gene of interest and in untreated planktonic samples unless specified. **(D)** Potential regulation of the *pyRG* gene by in *P. aeruginosa* by 3' end formation in its transcript leader. The *pyrG* expression is controlled by transcription attenuation in *B. subtilis* [5]. Genome browser image shows *pyrG,kdsA* operon. **(E)** Premature 3' end formation in *trpGDC* operon in *P. aeruginosa* biofilms. %ET values in planktonic (untreated and +AZM) and untreated biofilm samples were below the cut-off value. However, in AZM-treated biofilms (+AZM), regulation by premature 3' end formation was predicted. The gene is predicted to be regulated by transcription attenuation in *B. subtilis* [6]. **(F)** A closer view of the transcript leader and early termination peak in *trpGDC* operon. The 3' end peaks are located adjacent to a potential uORF with GTG start codon.

Supplementary Figure References

1. CLSI. Performance standards for antimicrobial susceptibility testing. Wayne, PA: Clinical and Laboratory Standards Institute; 2019.

2. Silke JR, Wei Y, Xia X. RNA-Seq-based analysis reveals heterogeneity in mature 16S rRNA 3' termini and extended anti-Shine-Dalgarno motifs in bacterial species. G3 (Bethesda). 2018;8: 3973–3979. doi:10.1534/g3.118.200729

3. Kaczanowska M, Rydén-Aulin M. Ribosome biogenesis and the translation process in *Escherichia coli*. Microbiol Mol Biol Rev. 2007;71: 477–494. doi:10.1128/MMBR.00013-07

4. Thomason MK, Voichek M, Dar D, Addis V, Fitzgerald D, Gottesman S, Sorek R, Greenberg E. A *rhlI 5′* UTR-derived sRNA regulates RhlR-dependent quorum sensing in *Pseudomonas aeruginosa*. mBio. 2019;10: 43. doi:10.1128/mBio.02253-19

5. Turnbough CL, Switzer RL. Regulation of pyrimidine biosynthetic gene expression in bacteria: Repression without repressors. Microbiol Mol Biol Rev. 2008;72: 266.

6. Du H, Tarpey R, Babitzke P. The *trp* RNA-binding attenuation protein regulates TrpG synthesis by binding to the *trpG* ribosome binding site of *Bacillus subtilis*. J Bacteriol. 1997;179: 2582–2586. doi:10.1128/jb.179.8.2582-2586.1997